Available online at www.sciencedirect.com
ScienceDirect
Solar Energy Materials & Solar Cells 92 (2008) 686–714
Solar Energy Materials and Solar Cells
www.elsevier.com/locate/solmat

Review

Stability/degradation of polymer solar cells

Mikkel Jørgensen*, Kion Norrman, Frederik C. Krebs

National Laboratory for Sustainable Energy, Technical University of Denmark, Frederiksborgvej 399, DK-4000 Roskilde, Denmark

Received 13 November 2007; received in revised form 3 January 2008; accepted 4 January 2008
Available online 10 March 2008

Abstract

Polymer and organic solar cells degrade during illumination and in the dark. This is in contrast to photovoltaics based on inorganic semiconductors such as silicon. Long operational lifetimes of solar cell devices are required in real-life application and the understanding and alleviation of the degradation phenomena are a prerequisite for successful application of this new and promising technology. In this review, the current understanding of stability/degradation in organic and polymer solar cell devices is presented and the methods for studying and elucidating degradation are discussed. Methods for enhancing the stability through the choice of better active materials, encapsulation, application of getter materials and UV-filters are also discussed.
© 2008 Elsevier B.V. All rights reserved.

Keywords: Degradation; Stability; Polymer photovoltaic; Organic solar cells; Mechanisms

Contents

*Corresponding author. Tel.: +45 4677 4717; fax: +45 4677 4791.
E-mail address: mikkel.joergensen@risoe.dk (M. Jørgensen).

0927-0248/$ - see front matter © 2008 Elsevier B.V. All rights reserved.
doi:10.1016/j.solmat.2008.01.005

1. Introduction

Research in the field of polymer and organic solar cells is still in an exciting phase with a rapid progression of improvements in the technique as detailed in a series of reviews [1–8] and special issues [9–13] with varying degrees of specialization. The reviews available range from generally addressing the field of polymer and organic solar cells [1–5] through reviews dedicated to low band-gap materials [6,7] and small molecule solar cells [8]. In the special issues [10,12], the field has been presented in a series of short articles with an overview nature [14–19]. In terms of research trends, the main direction has been towards the achievement of as high a power conversion efficiency as possible under simulated sunlight. The efficiency has reached 6.5% recently in a tandem cell [20]. The efficiency that can be reached with single junction cells is currently in the neighborhood of 5% [21,22] while the predictions of the theoretically and practically accessible power conversion efficiencies are indicated to be around twice that value or even higher [23–25]. As an area of focus, the power conversion efficiency is of course highly important in order to compete with the more mature silicon technology and justify research in an inferior technology (when considering the achievable power conversion efficiency). As with any discipline where hard numbers are compared competition between scientific research groups has the consequence that unrealistic or erroneous values are published. Sadly, 2007 was the year where such events cast a dark shadow over the field of polymer and organic photovoltaics. The only way out of this calamity is by independent verification or certification of groundbreaking results [26,27].

Aside from the power conversion efficiency, there is however at least two other important factors that will enter in the recipe for the success of polymer and organic solar cells, which is summarized in Fig. 1 as the unification challenge. To explain, Fig. 1 implies that research in any of the three areas of process, stability and power conversion efficiency will not necessarily lead to a useful technology as all three parameters are to some extent needed for this to be achieved. As long as the research focus is on just one of these areas progress towards application of the technology is anticipated to be slow as a breakthrough in one of the areas is very unlikely to automatically grant solutions in the other two areas (while serendipitous and fortuitous discoveries are naturally possible they are unlikely).

The important aspects other than the power conversion efficiency that have been identified are the stability, the cost and the processing [17,28,29]. These individual areas have been given relatively little consideration. Especially, the

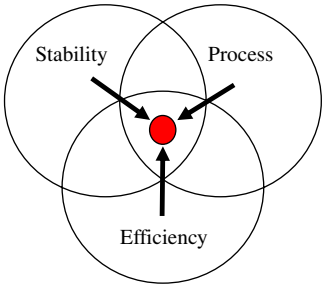

Fig. 1. The challenge of unifying efficiency, stability and process for the same material. The properties have been demonstrated individually but their combination has only been attempted in a few reports.

rather poor device stability of organic solar cells has been given little attention. Inorganic silicon-based solar cells may last on the order of 25 years; so in this respect, organic devices must be improved tremendously to become technologically interesting. Organic materials are by nature more susceptible to chemical degradation from e.g. oxygen and water than inorganic materials. A number of studies have been carried out and they show that the stability/degradation issue is rather complicated and certainly not yet fully understood though progress has been made. It is the aim of this paper to review the relevant literature up to this point and show how diverse the problem of device degradation really is. It has also been the intention to show the variety of investigative techniques that have already been applied. If polymer solar cells are to become more than a scientific curiosity, work in this area is highly needed.

This review has been organized according to the present understanding of the various degradation processes occurring in organic solar cells (Fig. 2). There is a rough division between chemical and physical degradation studies. Organic materials and metal electrode materials such as aluminum are susceptible to reactions with oxygen and water. There are subsections on the photodegradation of polymers, on polymer/oxide composites and on degradation at the ITO and metal electrodes. A small section is devoted to the rather unexplored physical degradation, mainly on the subject of morphology. Accelerated testing methods are described since they are required for some of the more stable devices that already exist. Furthermore, a section covers encapsulation techniques and getter materials. Finally, some suggested guidelines for recording and reporting stability and lifetime data are given.

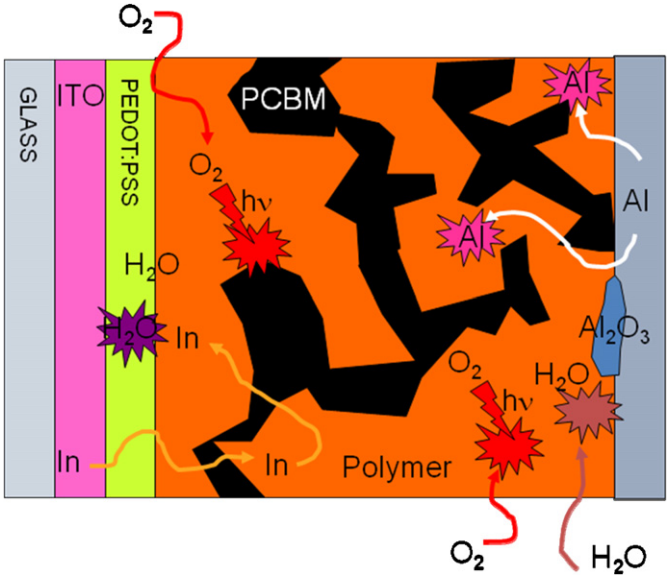

Fig. 2. Cross section view of a solar cell with the many processes that conspire to degrade polymer solar cells. A schematic illustration of some degradation processes that take place in a typical bulk heterojunction are shown.

1.1. Historical view of degradation in organic solar cells

While most early reports of stability and degradation in polymer organic photovoltaics date back to the beginning of the 1990s, the topic has from the beginning not been independent but has been included as footnotes in other studies or briefly mentioned in passing. The earliest example is perhaps by Yu et al. [30] from the group of A.J. Heeger that state the importance of degradation and stability and report preliminary data on the dark stability for devices kept in a glovebox over a period of 3 months. The illumination intensity used for the sporadic measurements of the efficiency was as low as 20 mW cm^{-2}. The authors in this paper also promised that a detailed study was under way but it has yet to be seen. From this point of view, it is problematic to find many of the reports, as they are fragmented and not readily searchable since the words rarely enter the title, abstract or keywords. An exhaustive list of these early pieces of information is thus impossible to provide while an overview is given in the following. There has also been a clear trend from these early reports to single observations without ties to the existing literature on stability and degradation where the issue has been addressed properly over a well-defined period of time and most often the experiment is described to the extent that the results are useful [31]. An absolute prerequisite is the knowledge of the incident light intensity, the spectrum of the incident light (i.e. AM1.5D or AM1.5G) [32], the manner of illumination (i.e. continuous, intermittent, short, only during *IV*-curves), the temperature of the device during the experiment, the atmosphere (i.e. humidity, oxygen content, glove box, vacuum etc). Furthermore, a lot of the work pertaining to the stability of OLEDs and PLEDs that was reported in the 1990s is highly relevant for polymer/organic photovoltaics. There are however, some important differences in the operation of these two types of devices that might change some of the contributing factors significantly.

The final and most recent trend is the detailed and deliberate study of the stability of the devices and of the chemical and physical degradation mechanisms. Testing of the lifetime can be standardized to allow direct comparison from different research groups. Efficiency measurements and solar simulation has been standardized for some time according to IEC and ASTM standards [33,34], though some ambiguity still exists in the literature. Similarly, lifetime measurements could be standardized so that it might be possible to compare studies from different research groups and industry.

Stability/degradation of polymer solar cells has not been reviewed previously as a separate issue, but has received attention in other reviews [35] (Scheme 1).

In contrast to the measure of power conversion efficiency, there is no single indicator for stability and for this reason most reports on stability employ different measures and different experimental conditions. It is thus impossible to directly compare stability reports due to the

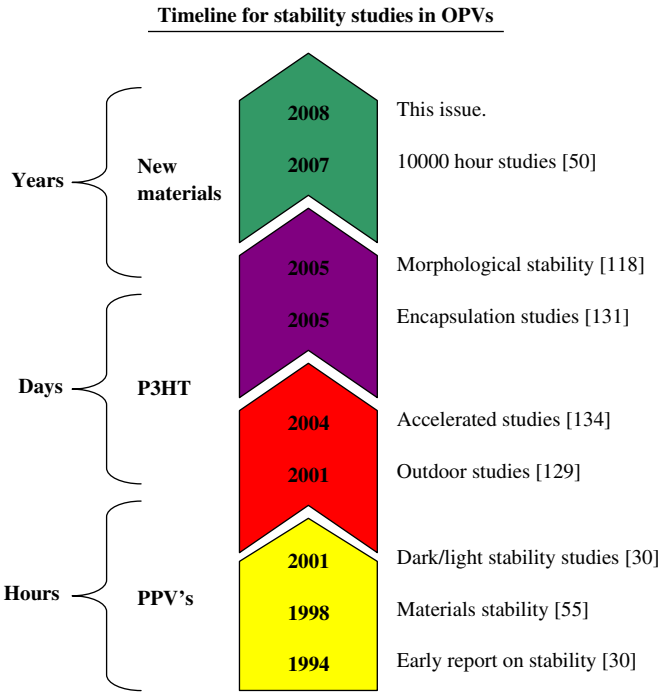

Scheme 1. A graphical overview of the field of stability and degradation of polymer solar cells. The lifetime under atmospheric conditions and the typical material is estimated on the left-hand side.

differences in materials, conditions, data acquisition, etc. We have however tried to create a graphical overview of the field of stability by highlighting a few reports that in our view changed the way of thinking.

2. Chemical degradation

2.1. Introduction

Chemical degradation of organic solar cells mainly focuses on the role of oxygen, water and electrode material reactions with the active polymer layer. Small amounts of oxygen and water can be introduced during the device fabrication absorbed in the different layers, but perhaps more importantly they can diffuse into the finished device.

Oxygen is readily activated by UV illumination in the presence of sensitizers such as titanium oxide or organic molecules. The superoxide or hydrogen peroxide formed will then aggressively attack any organic substance present including the active polymers. Some materials are more vulnerable to degradation than others, however, and the task is therefore to select polymers with desirable electro-optical properties that are also resistant to chemical and photochemical degradation. The previously popular PPV-type polymers such as the prototypical MEH-PPV and MDMO-PPV are especially prone to chemical attack and devices are typically degraded significantly in a matter of minutes to hours under $1000\,W\,m^{-2}$ illumination in ambient atmosphere. Poly-3-hexylthiophene (P3HT) is significantly more stable, but devices based on this material are also susceptible to chemical degradation.

When the solar cell performance is measured as a function of time a response curve is observed that may initially present improvement in performance, but that inevitably will decay. The decay curve may often be fitted by functions of linear or exponential character (Eq. 1) or may present a shape that can be fitted by a combination of functions. The decay curve naturally reflects the sum of all the processes that lead to degradation and may reveal mechanistic detail but this is by no means the general case. In one example of devices based on MEH-PPV an initial rapid deterioration followed by a more moderate decline was observed. This behavior could be fitted by using a second (or higher)-order exponential decay equation [36]. Stretched exponentials have also been employed for modeling the decay of the luminescence in OLEDs [37]:

$$\eta = a e^{-\alpha t} + b e^{-\beta t}. \quad (1)$$

The fast decay was shown to be independent on whether the device was operated in air or in nitrogen. It was proposed that this decay was associated with reactions at the polymer/aluminum interface. A thin barrier layer of vacuum deposited C_{60} between the polymer and the aluminum electrode retarded the fast decay. The second decay was however faster in the presence of air and therefore ascribed to the reaction with oxygen. It should be borne in mind that the decay curve measured as the short circuit current, open circuit voltage, fill factor (FF) or efficiency is a macroscopic device measurement that rarely will reveal microscopic detail of the processes leading to device degradation. Further, the least suited parameter for following the decay is the open circuit voltage.

2.2. Diffusion of oxygen and water into the OPV device

It is well known from experiments that the photovoltaic performance degrades faster if the OPV device is exposed to oxygen and/or water (i.e. ambient air). One of the earliest reports employed a simple layer of MEH-PPV sandviched between ITO and aluminum electrodes [38]. Such observations lead to the conclusion that oxygen and water diffuse into the device and react with the active materials in the OPV resulting in degradation of the photovoltaic performance. Detailed knowledge on the mechanism of transport and diffusion of oxygen and water into devices are urgently needed. A solid effort has been initiated by B.M. Henry that not only addressed the fundamental processes of oxygen and water diffusion through thin films, but also applied the knowledge in preparation of barrier materials and most recently also their application within the filed of polymer solar cells [39–43]. It is tragic that B.M. Henry passed away in the very beginning of a promising carrier and a great loss to the field. Encapsulation impedes the process, but the currently available materials used for encapsulation do not remove the process. Even if complex encapsulation schemes such as a sealed glass container [44] or a high vacuum chamber [36] are employed the overall device degradation is not stopped

while the processes involving water and oxygen are efficiently alleviated (Fig. 3). When oxygen and water are present, their diffusion into the OPV device is generally regarded as the dominant source of degradation. It is thus imperative to gain detailed knowledge of the mechanisms of oxygen and water diffusion into the OPV device. Norrman et al. developed a technique for isotopic labeling used in conjunction with imaging mass spectrometry [45] that was later applied for studying the degradation of polymer solar cells using $^{18}O_2$ [46–50] and $H_2{}^{18}O$ [51]. These experiments made it possible to map the oxygen/water diffusion process into OPV devices by detecting the reaction products. This was carried out by exposing OPV devices to isotopically labeled oxygen ($^{18}O_2$) or isotopically labeled water ($H_2{}^{18}O$) during either storing in darkness or illumination with a subsequent mass spectrometry analysis employing TOF-SIMS. It was found that oxygen and water diffuse through the outer electrode (counter electrode to ITO) [47–49]. Furthermore, diffusion through the sides of the device was found not to be an important entrance channel [48,50].

Diffusion through the outer electrode was shown mainly to proceed via microscopic pinholes in the electrode. Another possible entrance channel was proposed to be through the metal grains that evaporated electrodes typically consist of. It was shown for oxygen that the sublayer of organic material is oxidized and the material uptake (i.e. addition of oxygen) is causing the material to expand in all directions resulting in the formation of protrusions on the outer electrode surface centered on the microscopic pinholes in the electrode surface [47]. It was found (not surprisingly) that oxygen and water diffuse through the microscopic holes in the electrode surface regardless of whether the device is illuminated or stored in darkness. However, illumination was found to accelerate the oxidation of the sublayer of organic material. In addition, the authors have demonstrated that oxygen and water diffuse through all the layers in the OPV device (and react with them) until the counter electrode (ITO or an oxide) is reached where oxygen is exchanged on the ITO surface in the interface [48,50]. It is obviously important to minimize or remove the microscopic pinholes. No work has been published that deals with aspects of this phenomenon, e.g. why are these microscopic pinholes formed during the evaporation process and which factors will affect the density and size distribution such that the phenomenon can be controlled, i.e. removed or minimized? It is possible to prepare very smooth aluminum films by DC magnetron sputtering [52] whereas this technique is detrimental to the active layer unless special precautionary measures are made.

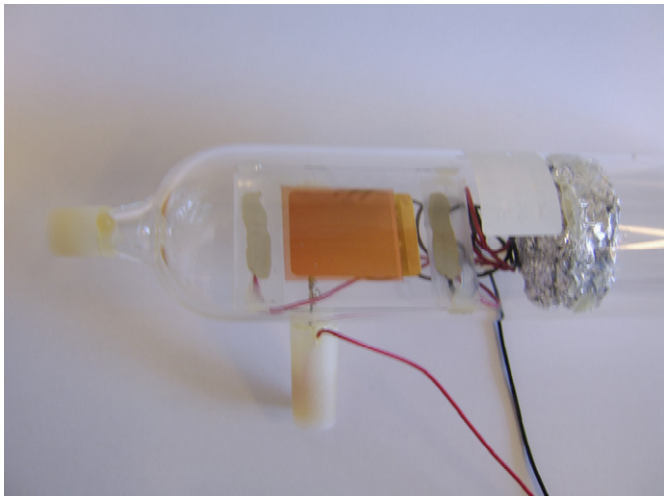

Fig. 3. A 10 cm^2 solar cell encapsulated in a glass ampoule sealed under high vacuum. The electrical connections to the inside of the ampoule are made using tungsten glass seals. The sealing procedure is laborious while the container is impervious to both oxygen and water. The white glued caps are protecting the glass seal and does not represent sealing itself. The aluminium foil is a heat shield necessary for the sealing procedure.

2.3. Photochemistry and photo-oxidation of polymers

Various PPV-type polymers have previously been very popular active materials for solar cells. PPVs are however susceptible to photo-oxidation resulting in a short lifetime of the devices. The mechanism of this chemical degradation is fairly well understood. Singlet oxygen is formed by energy transfer from the photoexcited polymer to adsorbed ground state oxygen molecules. Certain requirements are necessary: the triplet state (T_1) of the polymer must be higher in energy than the singlet state of oxygen for the energy exchange to take place (Fig. 4).

The intersystem crossing from the polymer S_1 to T_1 states must also be reasonably favored and the T_1 state has to be long lived enough to enhance the probability of the energy exchange. The singlet oxygen is then believed to react with the vinylene groups in PPVs through a 2+2 cyclo addition reaction. The intermediate adduct may then break down resulting in chain scission [53] (Fig. 5).

Dam et al. [54] investigated the singlet oxygen photo-degradation of oligomers of phenylene vinylenes as model compounds for the degradation of PPVs as shown in Table 1. They found that the rate of reaction with oxygen depends greatly on the nature of the substituents. Electron donating groups enhance the rate while electron withdrawing substituents retards the rate. Cumpston and

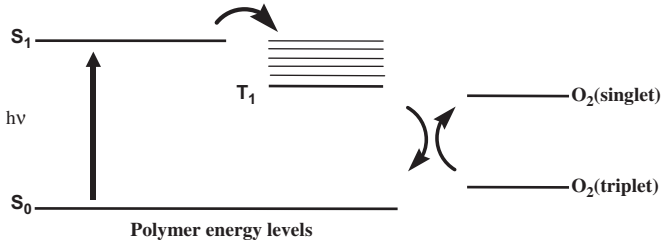

Fig. 4. Energy-level diagram of a polymer and oxygen (O_2). The first excited state of the polymer (S_1) can cross over to the triplet state (T_1), which can then transfer the excitation to adsorbed O_2, forming singlet oxygen.

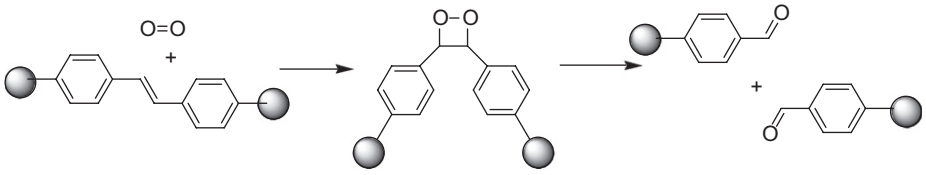

Fig. 5. Initial reaction of a PPV polymer with singlet oxygen. Singlet oxygen adds to the vinylene bond forming an intermediate dioxetane followed by chain scission. The aldehyde products shown can react further with oxygen.

Table 1
Relative rates of singlet oxygen degradation constants for substituted oligo-phenylene-vinylenes and a PPV [54]

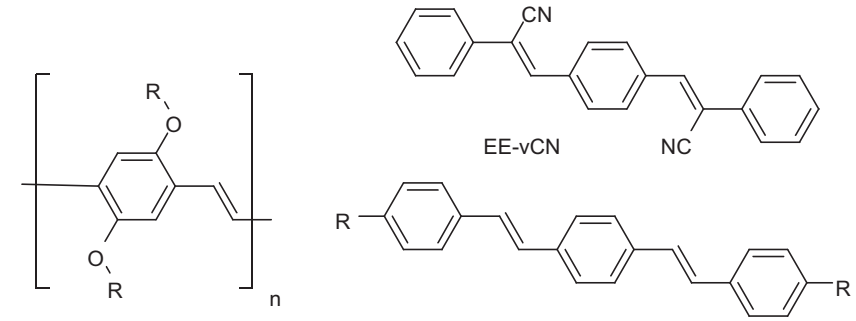

Molecule	k_{deg} (rel)
BCHA-PPV	8.0
EE-OCH_3	0.57
EE-CH_3	0.52
EE-CN	0.16
EE-vCN	0.01

Jensen [55] have studied the photo-oxidation of a series of OPVs and also some poly-(phenylene acetylenes) (PPAs) with infrared reflection absorption spectroscopy (IRAS). A film of the polymer (e.g. MEH-PPV) on aluminum was irradiated with an argon ion laser (514 nm) with an intensity of 10 mW cm^{-2} and IRAS spectra were taken at intervals up to 9 h. The IR bands corresponding to the different groups in the polymer and the photooxidized product were identified.

The most obvious change was the appearance of a broad carbonyl peak centered around 1740 cm^{-1} while peaks due to the vinylene group 969 cm^{-1} diminished simultaneously. The relative reactivities of three different OPVs were measured and it was found that MEH-PPV-CN and PPV-DP (see Fig. 6) was 76% and 45% less reactive towards singlet oxygen than MEH-PPV itself. Bianchi et al. [56] used elipsometry to investigate the photo-oxidation of MDMO-PPV films and the measured complex dielectric function ε^* (E) and complex refractive index $n^*(E)$ as a function of exposure to white light radiation (100 mW cm^{-2}). The results showed that the vinylene groups were oxidized to carbonyl groups.

Neugebauer et al. [57,58] investigated the photochemical degradation using Fourier transform infrared spectroscopy (FTIR). The area under the IR bands at 1182 cm^{-1} (C_{60}), 1506 cm^{-1} (MDMO-PPV) was measured as a function of time while the sample film was illuminated with an argon laser (488 nm, 30 mW cm^{-2}). A much faster decay of the MDMO-PPV component was observed reaching a plateau after about 3 h. When ambient air was substituted with argon no significant reduction in the IR bands were observed over 8 h. The authors concluded that the stability of the polymer part of the solar cell needed to be improved and that protective technologies such as additives and/or protective layers could be used. Padinger et al. [59] also studied the degradation of a bulk heterojunction MDMO-PPV/PCBM cell. The output current of the solar cell either in the dark or under white light illumination (80 mW cm^{-2}) and protected by inert gas was measured as a function of time.

A very rapid decay was observed for the cell under illumination as might be expected from previous work. The decay of the cell kept in the dark between measurements was also significant however and this decay was enhanced

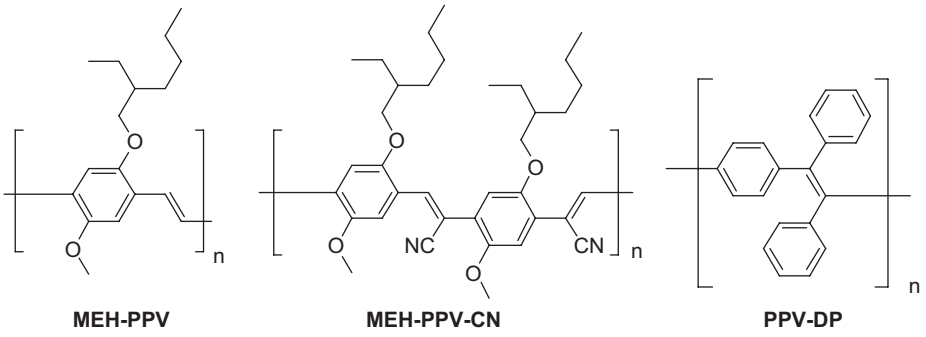

Fig. 6. Chemical structures for MEH-PPV, MEH-PPV-CN and PPV-DP as studied by Cumpston and Jensen [55].

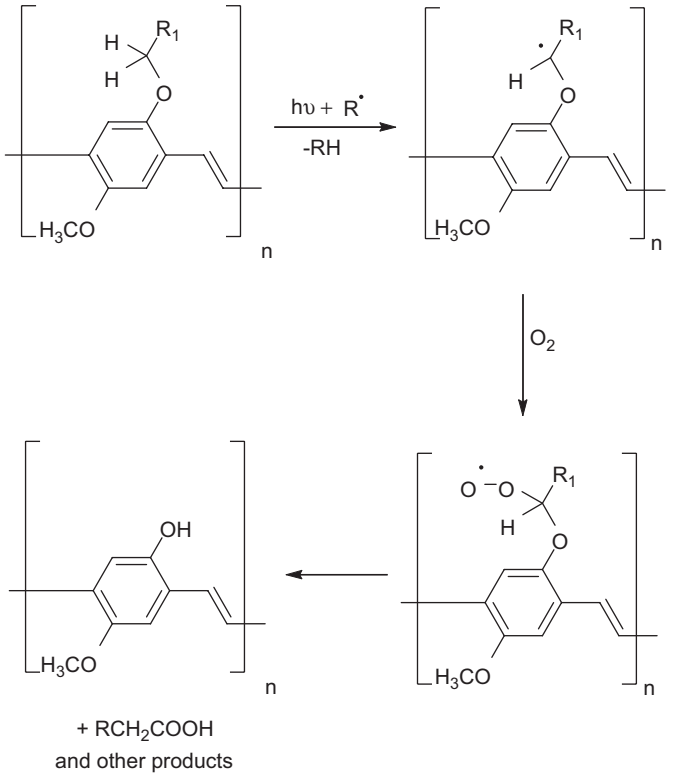

Fig. 7. Alternative light-induced oxidative degradation of MDMO-PPV involving the ether side chains.

greatly when the cell was kept at an elevated temperature of 57 °C. The underlying mechanisms for the degradation were not discussed in this paper, but the rapid degradation in the dark indicates that photo-oxidation is only one of several decay mechanisms and other mechanisms such as addition of aluminum to double bonds followed by reaction with water are equally likely. Chambon et al. [60,61] have used a combination of IR and UV techniques to elucidate the degradation mechanisms of the MDMO-PPV polymer. According to these investigations, oxidation of the ether side chains may predominate over direct attack of oxygen on the double bonds in the presence of large amounts of PCBM that efficiently quench the excited state whereby sensitization of singlet oxygen is suppressed. The carbon atom next to the ether oxygen of the side chain is especially susceptible to radical initiated oxidation as shown in Fig. 7. The specific degradation of the side groups could be followed by observing the IR band at 1352 cm^{-1} ascribed to the ether linkage. In the presence of oxygen, this band disappeared over a 100 h irradiation time. When PCBM was present however, this degradation was retarded by a factor of ten. It was concluded that PCBM protects MDMO-PPV by acting as a radical scavenger. If oxygen was excluded from the experiments a far more dramatic decrease in the rate of degradation of a factor of 1000 was observed. The authors proposed that the loss of photovoltaic properties were due to other degradation processes such as morphology changes or degradation at the interfaces.

Alstrup and Norman [62,63] studied photo-oxidation of a PPV oligomer as shown in Fig. 8 that was used as the active material in an OPV device. The molecule was equipped with end-groups that facilitate a mass spectrometric analysis (TOF-SIMS). The authors found the vinylene groups to be especially susceptible to photo-oxidation in agreement with what is described in the literature and discussed previously in this section. The unique part of the experiment was that it was possible to monitor the reaction/degradation of specific bonds in the molecule as a function of time. Fig. 9 demonstrates this for selected specific degradation processes. The implications of this finding is that the history of the cell or the age of the cell may determine which degradation processes that are taking place or dominate in the cell at any given time. The degradation mechanisms that are important for the degradation of the solar cell performance when the cell is freshly prepared may thus not take place at a later stage where other processes that were not preponderant in the beginning take over.

The reaction of P3HT with oxygen has not been investigated in any detail yet. It is known however, that poly(3-alkylthiophenes) form charge transfer complexes with oxygen shown in Fig. 10 [64]. The resulting cation and anion radical species can be detected by electron spin resonance and represents a doping of the polymer. It was found that a sample under vacuum contained 5.4×10^{17} spins g^{-1} (electrons). In oxygen (1 atm), the spin density increased more than ten-fold to 7.1×10^{18} spins g^{-1}.

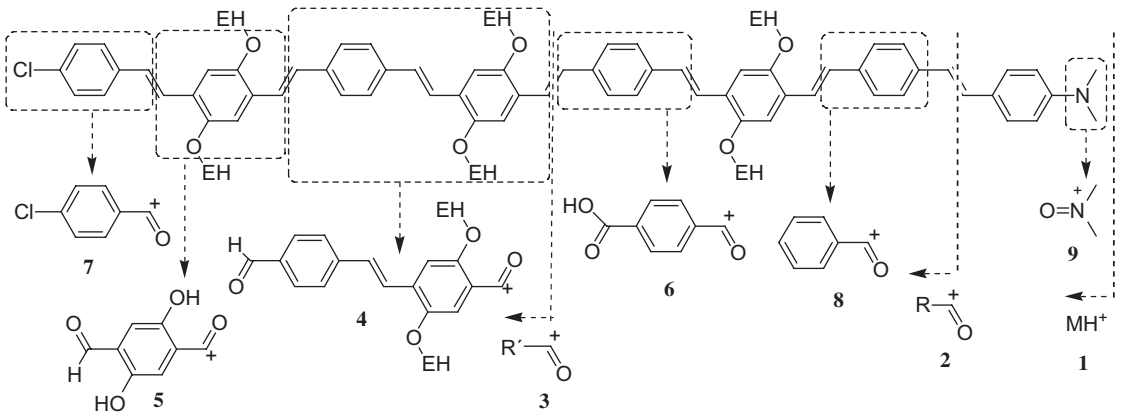

Fig. 8. Molecular structure of a PPV oligomer, proposed mass spectral fragment ions, and an indication of the possible origin of the proposed fragment ions. It should be emphasized that the fragment ions do not necessarily have the indicated molecular structures in the mass spectrometer.

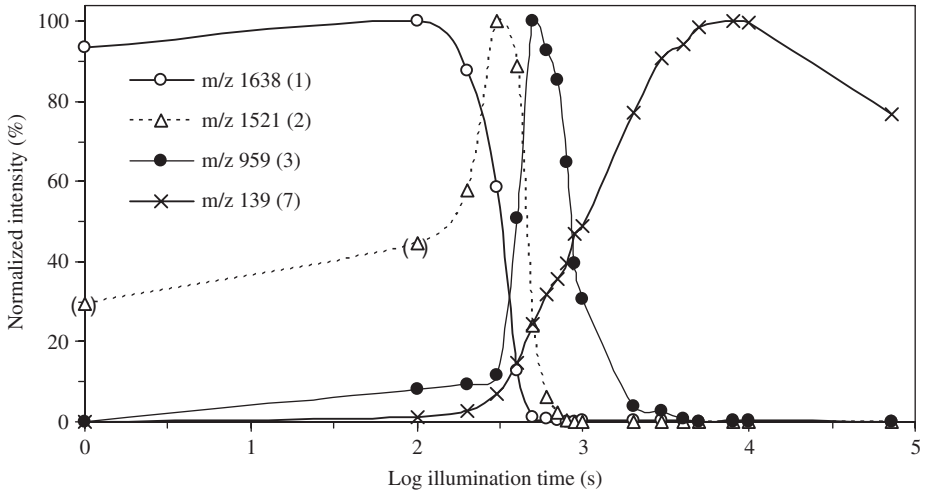

Fig. 9. TOF-SIMS normalized secondary ion intensities versus illumination time for the molecular ion and selected fragment ions from Fig. 8. The sum of all isotopes was used for the molecular ion. The points in parentheses are artefacts caused by mass spectral peak overlap. The small increase at m/z 1638 from 0 to 100 s is real and believed to be a subtle matrix effect caused by the increasing oxygen incorporation in the surrounding material.

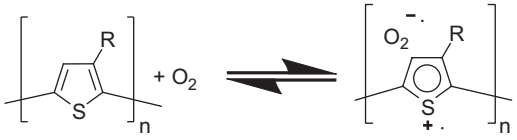

Fig. 10. Reversible formation of a charge transfer complex between P3AT (A = alkyl) and oxygen. R represents an alkyl group.

As a consequence the carrier mobility and conductance of P3HT films increased dramatically with the oxygen concentration.

The formation of charge transfer complexes between oxygen and P3HT is reversible but does not in itself lead to degradation of the polymer. Photosensitization of singlet oxygen by triplet states on P3HT seems unlikely due to the very low triplet quantum yield of this polymer. Alternatively, the authors speculate that singlet oxygen may be formed on dissociation of the excited state of the charge transfer complex.

The further reaction of oxygen with P3HT has not been investigated, but simple thiophenes react with oxygen at low temperature (−50 °C) under irradiation to form thioozonides, which undergo further degradation at room temperature as shown in Fig. 11 [65]. The reversible formation of complexes between oxygen and P3HT was investigated by oxygen-induced fluorescence quenching by Lüer et al. [66]. The diffusion coefficient of oxygen in P3HT was found to be $1.5 \times 10^{-7}\,cm^2\,s^{-1}$ and a fast reversible component of the fluorescence quenching leading to a loss of ca. 2% within milliseconds. A slower reversible component that depends on the light intensity occurs at the time-scale of minutes. The authors suggest that the slow reaction involves metastable oxygen species that are later responsible for the irreversible degradation of the polymer.

2.4. Degradation as a function of polymer preparation

In a lifetime study of MDMO-PPV-type polymer solar cells, de Bettignies et al. [67,68] investigated the effect of the

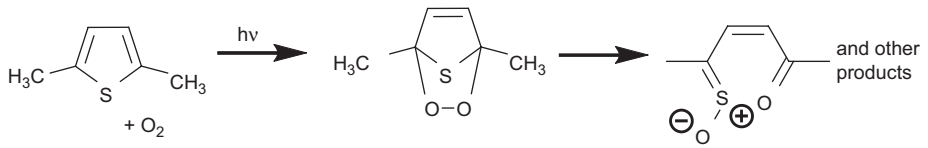

Fig. 11. Reaction between 2,5-dimethylthiophene and oxygen initially forming a thio-ozonide intermediate that can then decompose to an S-oxide and other products.

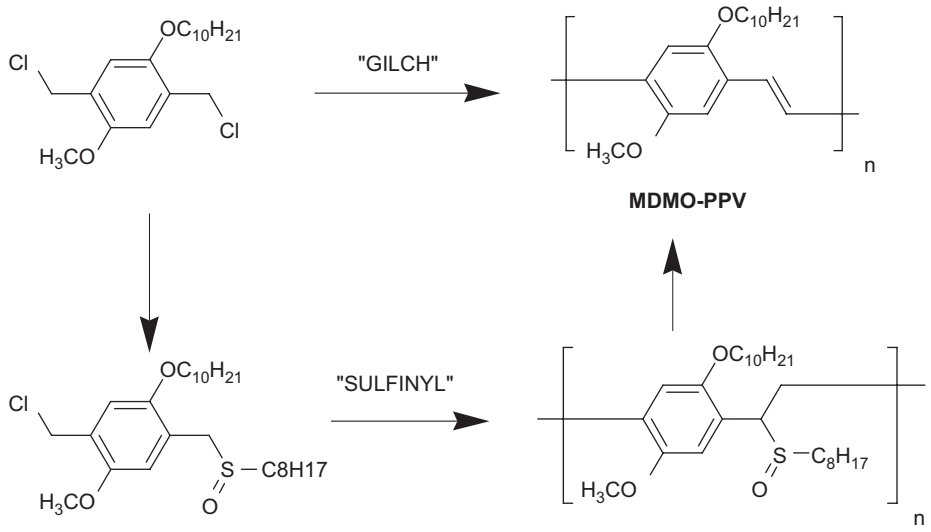

Fig. 12. The Gilch and the sulfinyl synthetic routes to MDMO-PPV.

route of polymer synthesis. Soluble PPVs can be prepared using a number of different synthetic routes. Two popular methods are the ''Gilch'' and the ''Sulfinyl''-type polymerizations outlined in Fig. 12. Devices of MDMO-PPV prepared by these two routes with PCBM had different *IV* characteristics and importantly, they also showed quite different decay of performance with time. While the devices based on the Sulfinyl PPV initially had a considerably higher efficiency η (2.46%) than that prepared from the Gilch-type polymer (1.10%) the Sulfinyl-based device decayed much more rapidly. In the time span investigated (0–120 h) both decays evolved roughly linearly with loss of efficiency of $0.013\%\,h^{-1}$ for the sulfinyl device and $0.003\%\,h^{-1}$ for the Gilch device. However, at all times the performance of the sulfinyl-based devices were superior. It is known from the literature that varying amounts (a few %) of impurities and defects are present in PPV polymers synthesized with these routes. The difference in the behavior could be due to this though a direct connection was not established.

The effect of the synthetic route was also observed for a dialkyl PPV prepared by three different routes [69], where the two routes employing palladium catalysis gave devices with low resistances due to metallic palladium nanoparticles. Similar differences could well exist for many other polymers and underlines the importance of purification of the polymers. The purification has been reported in a few instances, but this is far from being the general rule. Methods for for specific removal of transition metal impurities have been reported [70–72] using azothioformamides and the use of EDTA to remove nickel from polymers prepared using the Yammamoto reaction has also been reported [73].

2.5. Photo-oxidation in inorganic oxide/polymer nanocomposite films

Titania nanoparticle powders are used as electrodes in the Grätzel solar cell [74] and various types of organic solar cells. The same material is also used as the active component in self-cleaning windows where it takes part in a photocatalyzed oxidation of organic materials that adhere to the surface. In the presence of oxygen, there is therefore a competition between the extraction of the charge carriers in these solar cells and the reaction with oxygen and degradation of the organic components. In the Grätzel-type cells, the charge separation is extremely fast and the oxidation of the organic dye is not a problem.

Durrant et al. [75–78] have shown that UV illumination of TiO_2 powder results in photogeneration of an electron–hole pair. The electron is very efficiently transferred to bound oxygen (O_2) to generate the superoxide radical anion $O_2^{\bullet -}$, which, in turn, can oxidize many organic compounds including polymers. The photogenerated holes can react with surface hydroxyl groups to produce $TiOH^{\bullet +}$ that again can react and degrade adsorbed organic compounds. Transient absorption data exciting the sample with laser light with a wavelength of 337 nm and

a probe wavelength of 800 nm, under anaerobic conditions, showed a fast decay in the presence of an oxidizable species (methanol). In the presence of oxygen (unsealed sample), a 50-fold increase in the rate was observed. First-order rate constants of 70 and 1.4 s^{-1} were measured. Durrant and co-workers have developed film-type materials of polymer titania composites as photocatalytic oxygen-scavenging materials for use in packaging. Durrant et al. also reported hybrid solar cells based on TiO_2 and various conjugated polymers [79–82]. While no lifetime data or mention of stability was given for these hybrid cells, it is likely that photo-oxidation of the conjugated material took place leading to device degradation vis-à-vis Refs. [75–78].

Interestingly, some of the hybrid solar cells are based on mixtures of the inorganic semiconductor oxides such as TiO_2, ZnO, SnO_2, Nb_2O_5, CeO_2 and CeO_2–TiO_2 and the same phenomenon of photo-oxidation catalyzed by the oxide should be observed. Their efficiency and lifetime depend on oxygen and UV-irradiation in a complicated way. Lira-Cantu et al. investigated the solar cell diode characteristics and lifetime with respect to these factors with devices made up from the oxides TiO_2, Nb_2O_5 or ZnO in a bilayer structure with the organic polymer MEH-PPV [83,84]. Oxygen was found to be critical to the performance of the solar cells. Only in the presence of air, was there a significant short-circuit current J_{SC}. Lifetime studies showed a rapid decrease in J_{SC} when the devices were tested in an argon atmosphere or in vacuum. If oxygen was then admitted partial recovery of solar cell performance was observed. Irradiation with UV-light resulted in irreversible degradation and photobleaching of the polymer. Applying a UV-filter with a cut-off at 400 nm retarded this degradation, but did not inhibit it totally. In general, a short-term improvement of the current density is observed for all these hybrid solar cells working in air followed by a slower decay due to degradation of the polymer. The use of a UV-filter has been reported as beneficial for the stability in hybrid solar cells based on MDMO-PPV and zinc oxide nanoparticles [85].

A later study with isotopic labeling using $^{18}O_2$ showed that oxygen diffuse throughout the cell and is incorporated in the semiconductor oxide layer (Nb_2O_5) under illumination. This ''breathing'' was linked to the performance of the solar cell [48].

The interaction with oxygen and water in hybrid solar cells is by no means clear at present. For instance, in the case of hybrid cells based on zinc oxide some results seem to indicate that oxygen (and/or possibly water) is needed in an annealing step [86] for the devices to work well in air [83,86] while other reports achieve operation in the absence of oxygen [87].

2.6. Chemical degradation of the metal electrode

Aziz et al. [88–90] have investigated degradation mechanisms for organic light-emitting diodes (OLEDs) and they concluded that the major cause of degradation was due to (at least) three independent processes. Among the most relevant ones for solar cells are electrochemical reactions at the ITO and aluminum electrodes. It was also stated that the inclusion of moisture and impurities within the polymer will enhance ionic conduction and hence accelerate corrosion. Finally, it was found that illumination of the device will also accelerate degradation.

A theoretical investigation of the PPV aluminum interface has been carried out by Lögdlund et al. [91] proposing a direct reaction with the formation of Al–C bonds as shown in Fig. 13. It is the low work function of aluminum that makes it useful as the negative electrode material in solar cells and it also results in the high reductive power. The proposition of such a mechanism has its roots in the experimental observation of the reaction between PPVs and alkali metals [92,93] or aluminum [94]. Further, both interface and bulk-related defects have been linked to the degradation of OLEDs [95]. This reactivity has been recognized for a long time in organic chemistry where aluminum metal has been used for reduction via electron transfer to organic compounds (i.e. the Clemmensen reaction). An alternative to aluminum–carbon bonds as proposed by Lögdlund et al. would therefore be single-electron transfer with the creation of anion radicals on the polymer. In any case, both organo-aluminum compounds and anion radicals are highly reactive species that will react with any proton donors present or oxygen. One such proton donor could be traces of water introduced in the production of the device e.g. from PEDOT:PSS. The end result would be reduction of the vinylene groups to e.g. saturated bridges with the loss of conjugation in the polymer. This has however not been demonstrated directly by any characterization techniques. One special case is that of calcium where it has been shown that it only reacts with water at room temperature [96]. Metallic calcium electrodes will thus not react with molecular oxygen under dry conditions. Organocalcium compounds formed by addition of calcium to organic compounds however will react with oxygen vis-à-vis the discussion of aluminum above.

PCBM (and other fullerenes) have a very high electron affinity and would seem more prone to reaction with the metal electrode. C_{60} reacts with alkali metals to form compounds like K_3C_{60}. A similar reaction could be envisaged at the interface between PCBM and the aluminum electrode though this has not yet been demonstrated.

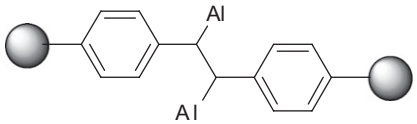

Fig. 13. Proposed structure of how part of the PPV structure may react with aluminum according to Lögdlund et al.

Melzer et al. [97] measured the *C–V* characteristics of ITO/PEDOT:PSS/MEH-PPV/C60/Al-type devices and found that a depletion layer formed at the C_{60}/metal interface with a dipole contribution of ca. 0.3 eV. The C_{60} layer was most likely n-doped with a low doping concentration of $10^{16}\,cm^{-3}$. Nishinaga et al. investigated co-evaporated films of C_{60} and aluminum and found evidence for direct metal-C_{60} interactions. The normally symmetry forbidden HOMO-LUMO transition became allowed presumably due to molecular distortion induced by the Al–C_{60} bonding [98]. The interaction between aluminum and C_{60} at the interface has been found to play a dominant role when it comes to charge transport across the interface that is not efficient unless there is a buffer layer [99] or the C_{60} is slightly doped.

A common practice with organic solar cells and OLEDs is to deposit an ultrathin barrier layer of Al_2O_3 [100,101] or lithium fluoride [102,103] between the polymer and the aluminum electrode. The effect of this layer on the performance of plastic solar cells has been studied by Brabec at al. [103]. Four main factors were presented: (i) the effective work function is lowered; (ii) reaction between aluminum and the polymer is eliminated; (iii) a dipole layer is formed and (iv) the polymer layer is protected from hot alumina during thermal evaporation of the metal. In general, an increase of the open circuit voltage (V_{oc}) and the FF was observed enabling a white light ($800\,mW\,cm^{-2}$) efficiency (η) of 3.3%. The formation of AlF_3 at the interface have been proposed but disproved [104]. Others have observed an improvement in the open circuit voltage (V_{oc}) with the introduction of a thin aluminum oxide layer at the organic/aluminum interface. [105] While these observations [98–105] do not report a link to device stability or to device degradation the implications of these findings does when considered in the context of other work on degradation and stability of solar cells. Improvements of the operational stability for devices employing a C_{60} layer between the aluminum cathode and the active layer has been reported [36] and very long lifetimes under accelerated conditions have been shown [50,106]. While the stability in the latter case has been suggested to be due to a particular hardness of the active polymer layer recent studies employing isotopic labeling and solid-state NMR indicate that hydrogen-bonded networks in the solid state may possibly be involved [107]. Interestingly, the pure aluminum–C_{60} interface should not work well in terms of charge transport unless an insulating layer is present at the interface unless the C_{60} is doped. It is possible that this layer is formed during preparation from traces of Al_2O_3 or that it forms quickly in situ when the devices have been prepared. Reactions at the aluminum interface may lead to a p-doped region in the polymer/acceptor layer with higher conductivity affecting the rectification behavior and diode characteristics (a Schottky diode). Glatthaar et al. [108,109] showed that this p-doping can be, at least partly, removed by annealing the finished device. Impedance spectroscopy showed that the semiconductor is divided in a low- and a high-conducting region. This method gives the capacitance of any RC elements in the device. The thickness d of the region giving rise to the capacitance can be estimated from Eq. (2):

$$d = \varepsilon_0 \varepsilon A / C. \tag{2}$$

A first annealing step at 110 °C for 30 s with 1 V bias gave rise to a capacitance feature with a thickness of 50 nm. A second annealing step at 110 °C for 450 s increased d to 100 nm. Another interface problem is corrosion at the aluminum electrode. In a second paper, Glatthaar et al. showed how this manifests itself in the appearance if the *IV*-curve of the photodiode [108] (Fig. 14).

This effect has also been observed to appear gradually during long lifetime measurements [50]. Devices with a poor FF show an inflection point in the *IV*-curve. This is seen as a kink in the curve in the fourth quadrant and has been interpreted as a counter diode. Impedance spectroscopy of such a device revealed a region of slow charge transfer, which was explained as a corroded aluminum interface. The implications of the work by Glatthaar et al. are far reaching and numerous literature reports show *IV*-curves, where the inflection behavior is present while it is rarely given mention. Other studies in support of the formation of an interface layer at the aluminum organic interface are the work by Paci et al. that studied operating bulk heterojunction solar cells based on MDMO-PPV and PCBM in situ using X-ray reflectometry [110,111]. The authors demonstrated changes in the reflectometry during continuous operation for around 1 day in an unspecified

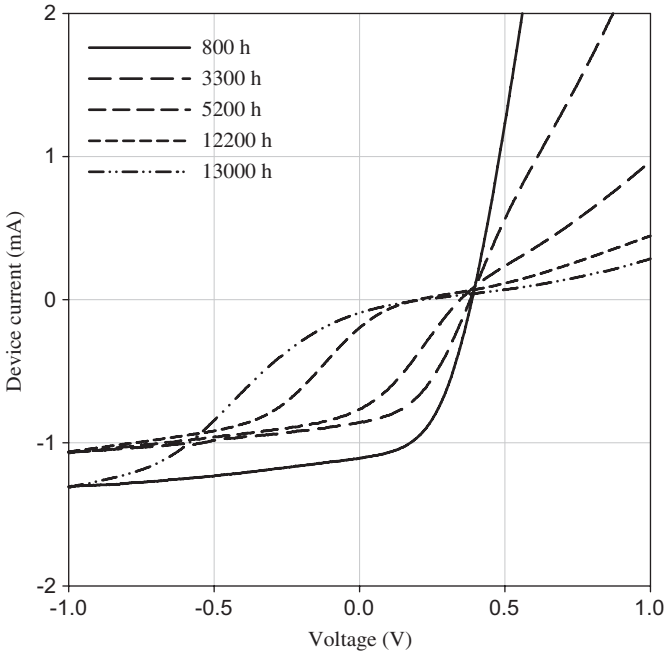

Fig. 14. *IV* curves of a P3CT/PCBM device taken at various intervals during a lifetime study. The normal diode characteristics are slowly replaced by a curve with a deflection point severely decreasing the device performance.

inert atmosphere. These changes were linked to a growth of the layered structure and explained through formation of an interface layer between the aluminum electrode and the organic layer. The application of an interfacial layer of LiF inhibited this effect. Recent results employing synchrotron work on heterojunction devices based on both MEH-PPV and P3HT mixed with PCBM confirm that changes do take place, but raise concerns as to whether X-ray reflectometry is suitable for characterization of the typically rough interfaces of bulk heterojunction devices [112]. The reactions at the aluminum–organic interface have been confirmed unequivocally in many studies employing isotopically labeled oxygen and water [36,46,47,49–51]. From this point of view, the use of solar cell geometries with a low work function metallic cathode is likely to have significant degradation mechanisms and instability linked to the reactive metal and the interface with the organic. While many of these tribulations may be circumvented by removal of water, oxygen and by the application of suitable interfacial barrier layers we identify the use of metallic low work function cathodes as problematic when it comes to manufacturing polymer/organic solar cells with long operational lifetimes unless the operation takes place with an efficiently encapsulated device or vacuum conditions are employed.

2.7. Chemical degradation of the ITO electrode

The stability of the interface between indium–tin oxide and PEDOT:PSS have been studied by de Jong et al. with the Rutherford backscattering (RBS) technique [113], which provides information on the atomic composition. Samples on glass slides with ITO/PEDOT:PSS/PPV were stored in a nitrogen atmosphere at 100 °C for up to 2500 h in the dark. RBS measurements of the PEDOT:PSS layer showed the indium content increased from 0.02% to about 0.22%. When samples were exposed to ambient air a much faster erosion of the ITO film occurred. A film stored at 8 °C in air had 1.2% indium in the PEDOT layer after 10 days. It was concluded that the ITO/PEDOT interface is very sensitive to air and that the hygroscopic nature of PSS allow absorption of water that facilitate etching of the ITO layer. Krebs and Norrman [50] observed ITO etching indirectly by observing indium diffusion into the layers in an OPV device with the composition Al/C_{60}/P3CT/ITO, where P3CT is poly(3-carboxythiophene-co-thiophene). The surprising observation was the fact that indium diffuses through all layers in the device and ends up on the outer surface of the counter electrode (aluminum). It is uncertain to what extent indium is involved in degradation processes when it diffuses through the organic layers of the device.

2.8. Degradation of the PEDOT:PSS layer

PEDOT:PSS or poly(ethylenedioxythiophene) poly(styrene sulfonic acid) is used as a hole transporting layer between the ITO electrode and active layer. It is usually purchased as a somewhat ill-defined solution in water and spin-coated onto the substrate followed by drying. Kawano et al. studied the effect of the PEDOT:PSS layer on degradation of MDMO-PPV:PCBM solar cells and found a large difference when cells were exposed to humid versus dry conditions [114,115]. Rapid degradation were evident in the cells illuminated under humid conditions (>40% RH) either in air or in nitrogen. Cells prepared without the PEDOT:PSS layer degraded relatively slower. The authors' conclusion was that the hygroscopic PEDOT:PSS layer takes up water from the atmosphere increasing sheet resistance. Only relative values for the efficiency of most of the cells tested were reported, however, so direct comparisons may be difficult. The time span used in these experiments was also limited to 8 h with cells degrading to 50% of the initial efficiency over 1–2 h.

Norrman et al. [47] made an observation that had not been described before in the literature regarding the PEDOT:PSS layer. The authors observed particle formation in an OPV device with the configuration Al/C_{60}/C_{12}-PPV/PEDOT:PSS/ITO. The particles are visible from fluorescence microscopy images of the active area after the aluminum electrode had been removed. The particles were also observed to form over time on a partial device composed of C_{12}-PPV/PEDOT:PSS/ITO. Based on a mass spectrometric analysis of these particles a molecular structure was proposed that enabled a mechanism of particle formation to be proposed (Fig. 15).

PSS is present in excess amount compared with PEDOT and can thus diffuse to other parts of the device, i.e. to other layers and possibly react with other components of the device. The authors suggested that PSS undergoes a so-called oxido-de-sulfonato-substitution forming the phenolate that can subsequently react with PSS forming two PSS chains linked together via a sulfonic ester group. Oxidation of the carbon indicated by an asterisk in Fig. 15 will then consequently form the proposed molecular structure of the particles observed. Like many other observed phenomena in OPVs, it is uncertain to what extent particle formation contributes to the overall device degradation. Furthermore, PEDOT:PSS is available from many sources and the different suppliers employ unspecified additives that are present in varying amounts.

2.9. Polymer materials for very stable solar cells

Essentially, only a few categories of conjugated polymers have been examined so far for stability in solar cells mainly the PPVs and P3HT. P3HT-based cells are superior by perhaps an order of magnitude or more in lifetime, presumably due to the lack of easily oxidizable vinylene groups. Another significant improvement in stability was found with solar cells made from P3CT. This polymer in itself is insoluble and hard. It is prepared in situ by thermocleavage from the soluble polyester derivative as shown in Fig. 16.

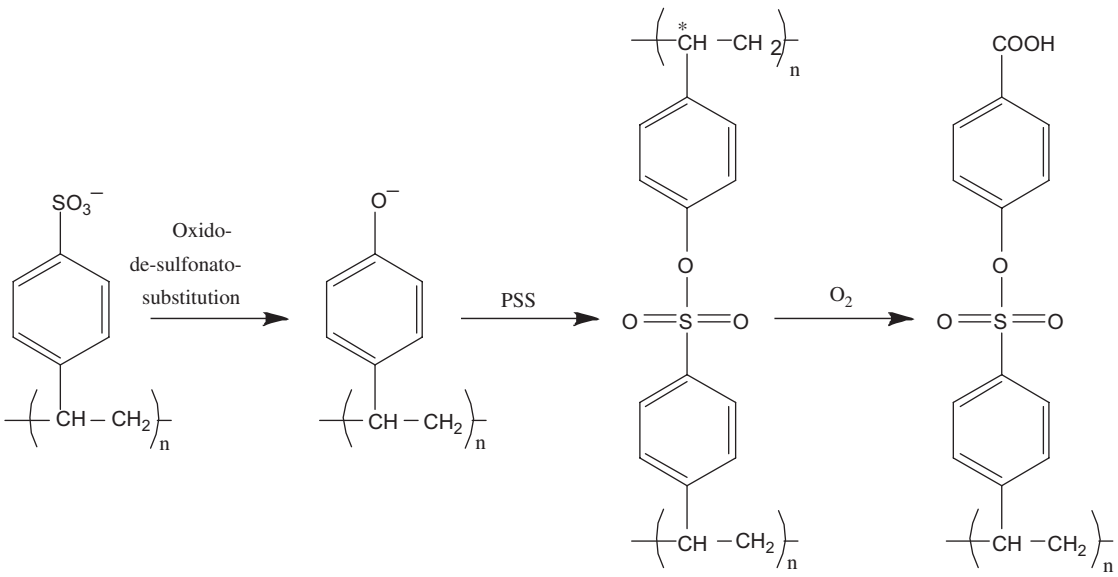

Fig. 15. Oxidative degradation of polystyrene sulfonic acid (PSS) in PEDOT:PSS. The asterisk indicates the carbon most susceptible to oxidation.

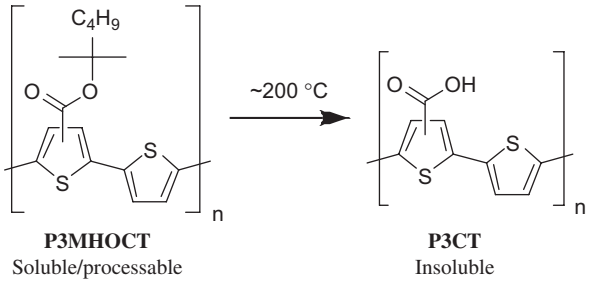

Fig. 16. Synthesis of the P3CT polymer for stable solar cells.

This polymer was originally synthesized by Liu et al. [116] to act as an interface layer between the TiO_2 electrode and P3HT in a hybrid cell. Later it was found that this polymer could be used to prepare very stable solar cells [106] with a lifetime in excess of 10,000 h under full sun (AM1.5G), high temperature and with exclusion of oxygen and moisture [50,117]. A comparative study between devices based on the soluble precursor P3MHOCT and P3CT showed that while the former devices degraded rapidly over a few hours, virtually no decay was observed for P3CT [117]. Since then prolonged degradation studies have shown that P3CT-based devices do decay albeit at a much slower rate than P3HT devices. A possible explanation for the longevity is that P3CT is a very hard material that may retard diffusion. It is however not so simple to replace P3HT by P3CT since it is synthesis requires a high-temperature cleavage step of about 200 °C after the film has been made. This step is not directly compatible with the formation of a bulk heterojunction with PCBM where temperatures up to a maximum of ~160 °C are employed when creating bulk heterojunctions of P3HT and PCBM. Devices based on P3HT–PCBM heterojunctions that were stable during 1000 h of accelerated testing under inert atmosphere have been reported [118].

2.10. Stability and lifetime reports

There have been some studies reporting the stability of devices under ambient conditions without encapsulation or with simple mechanical protection of the active layer with no barrier properties. All of these studies report a relatively short lifetime [119–127]. Studies employing either inert atmosphere during characterization or encapsulation have also been reported [128–130] and further studies reporting the dark stability of devices encapsulated in a flexible barrier material [131–133]. Finally, accelerated studies where the devices are subjected to extra stress in the form of high temperatures, high incident light intensities and continuous illumination are beginning to receive attention [134,135]. For OLEDs, electrical stress has also been employed [136].

2.11. Air stable polymer solar cells

The most desirable of all characteristics in the context of stability is operation of the device in the atmosphere without any form of encapsulation. The reason for this being that any combination of materials in a device that achieves this will have solved problems of stability and degradation that house the key to future developments. Unfortunately, very few such studies have been reported. In one study, an inverted cell geometry was employed with a gold anode giving devices with an operational stability of 2 weeks while it is not clear from the work if the illumination was continuous [137]. The authors have confirmed that the devices were left in the dark between measurements (private communication). There has so far been one study that reports a reasonable storability in

ambient air without any form of encapsulation and continuous operation in air at 1000 W m^{-2}, AM1.5G, 72±2 °C, 35±5% relative humidity for 100 h to 80% of the initial performance. Testing under the same conditions at a lower temperature of 30 °C gave much longer operational lifetimes [138]. Common to the two studies is that a relatively inert metal electrode is employed. In the latter case, the preparation was demonstrated by all solution processing in air (i.e. no vacuum steps).

3. Physical and mechanical degradation

3.1. Introduction

The physical degradation of organic solar cells has not been studied in any detail yet. It is clear that the device efficiency depend critically on the spatial organization of the different materials into layers with a precise thickness tailored for optimum photon harvesting and charge-carrier transport. In the bulk heterojunction cells, a further requirement is the nanophase separation of the active layer into an interpenetrating network of donor and acceptor material. The best methods for obtaining this structure/morphology have been at the center of OPV research for a number of years. It is now clear that this structure is not static once it has been formed during production of the device. Small organic molecules like PCBM and even polymers like P3HT may still have some freedom to diffuse slowly or recrystallize over time especially at elevated temperature. The best structure for device performance will in all probability not be the thermodynamically most stable. These gradual changes in the microstructure will lead to a degradation of the performance of the OPVs. This type of physical degradation is harder to study because we need methods to map the internal three-dimensional (3D) structure and to correlate this with device performance. Different types of microscopy have been used to gain insight into the size distribution of PCBM crystallites as a function of heat treatments (annealing).

3.2. Morphology control and morphological stability

The invention of the bulk heterojunction organic solar cell by Heeger et al. [139] increased the efficiency from the ca. 1% obtainable with single junction cells to the ca. 5% record of today [21,22]. The exciton diffusion range in the organic material is of the order of 10 nm limiting the optimum size of the polymer domains. At the same time, the charges that are created at the interface between the donor and acceptor must have continuous paths to the outer electrodes. This is solved in the bulk heterojunction cell with the creation of an interpenetrating network of electron donor (polymer) and acceptor (PCBM) materials. It is, however, not obvious how to obtain the optimal nanophase separation in the final device since it is probably not the thermodynamically most favorable geometry. Rather it depends on the kinetics of segregation and crystallization of the components. In most cases, a polymer/PCBM solution is spin-coated onto a substrate and many parameters such as the exact choice of solvent, concentration, ratio of donor and acceptor, temperature and particulars about the spin-coating itself come into play. The optimum morphology may be further developed through the process of annealing where the mobility is increased by heating the device for a short time to allow further migration and crystallization. Much of the improvements in efficiencies of organic solar cells have come from this very experimental adjustment of the fabrication process of the devices rather than from theoretical breakthroughs.

The phase segregation of MDMO-PPV/PCBM mixtures has been studied by Yang et al. in detail [140]. It was found that the PCBM aggregates and form microcrystallites that grow larger over time. The effects of thermal ageing have also been studied [141]. This annealing process, normally increase the short circuit current, but as the authors note "the thermal stability of MDMO-PPV:PCBM films will likely limit the long-term performance of solar cells based on these materials." They link the morphology changes to the rather low glass-transition temperature (T_g) of MDMO-PPV and also note that higher-T_g materials such as P3HT may increase stability of the devices. A combination of AFM and X-ray diffraction techniques were used by Kline et al. [142] to investigate the effect of polymer molecular weight of P3HT on morphology. Small molecular weight P3HT form a mesh of rod-like structures while high molecular weight P3HT is more homogeneous. The more ordered small molecular weight P3HT had a lower hole mobility explained by trapping of the carries in the ordered domains that are poorly connected. Similar fibril-like P3HT crystallites were observed by Klimov et al. [143] (Fig. 17) and by Yang et al. [118] in P3HT/PCBM mixtures and their conclusion was that annealing devices at 120 °C resulted in a stable morphology with device lifetime in excess of 1000 h at 70 °C under 1 sun illumination [118]. Yang and Loos have also reviewed the topic of morphology of blends relevant for solar cells [144]. Fibrillar structures have also been reported by Berson et al. and applied in bulk heterojunction solar cells without the need for thermal annealing to reach a stable nanostructure [145].

Enhanced thermal stability of the morphology and hence the device performance have been reported for a variation of P3HT copolymerized with a small amount (~4 mol%) 3,4-dihexyl-thiophene [146]. The dialkyl monomer introduces a slight disorder and lowers the regioregularity of the material. Devices based on this copolymer formed stable nanophase separated bulk heterojunction structures on short-time annealing (30 min, 150 °C) seen by transmission electron microscopy. The authors surmise that the high device efficiencies obtained with commercial P3HT of 5% may be due to a fortuitous lower regioregularity.

4. Characterization methods for investigation OPV of degradation

In order to prevent or at least minimize the undesired degradation of the OPV device, it is a prerequisite to be able to map the various degradation mechanisms and understand them. This can be achieved by employing a series of physical and chemical methods to study the OPV degradation. Table 2 lists useful and relevant techniques for studying degradation mechanisms in OPVs, and, in addition, lists relevant information associated with each method.

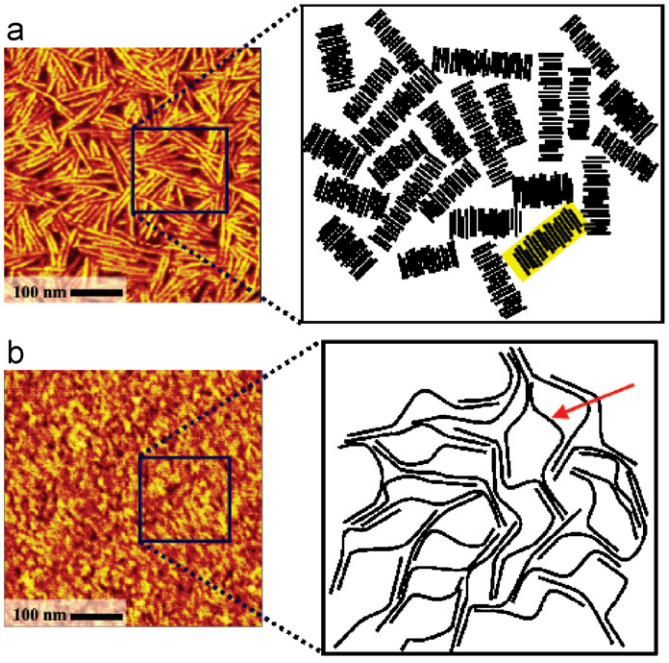

Fig. 17. Atomic force microscopy images of low-MW P3HT (top left) and high-MW P3HT (bottom left), (a) and (b) respectively. On the right is shown the authors interpretation of the structure as isolated nanorods (top right) and a more uniform high-MW film with better contact between ordered domains. (Reproduced with permission from ACS.) [143].

Since OPVs are multilayered devices it is important to have techniques that can perform depth profiling to study the degradation of each layer over time. Ideally, high-resolution in-situ 3D imaging of the chemical composition as a function of time could resolve many of the mysteries of the degradation processes. Such a technique is however not available and while 3D imaging can be obtained it is currently achieved by a combination of techniques and the methodology is destructive. It is thus not possible to test a device to a certain level, acquire a 3D image of the state of the device and continue testing afterwards to the next level. It is however possible to carry out a series of parallel experiments and then sacrifice one of the experiments each time a sample is needed. The most powerful technique currently that give a chemical 3D image is a mass spectrometric technique such as TOF-SIMS that have already been used for a number of such studies [129–131]. XPS also allow for 3D imaging and gives chemical information that albeit is somewhat more limited in chemical detail as compared with TOF-SIMS.

4.1. Methods based on device operation

Many of the techniques listed in Table 2 are limited to give information from the entire device. The electrical measurement of the device operation is such a measurement that only allow for the monitoring of the macroscopic

Table 2
Useful and relevant techniques for studying degradation mechanisms in OPVs and relevant information

Technique	Bulk analysis	Surface analysis	2D imaging	Depth profiling	Destructive analysis	Non-destructive analysis	Chemical information	Morphological information
IV-curves	●					●		
IPCE (EQE) measurements	●					●		
Impedance spectroscopy	●					●	(●)	(●)
UV–vis spectroscopy	●				(●)	●	●	(●)
IR spectroscopy	●				(●)	●	●	
X-ray reflectometry	●				(●)	(●)		●
RBS	●				●	(●)	●	(●)
TOF-SIMS		●	●	●	●		●	(●)
XPS		●	●	●	●		●	(●)
AFM		●	●		●		(●)	●
SEM		●	●		●			●
Interference microscopy		●	●		●			●
Efficiency 2D-imaging	●		●			●	(●)	(●)
Fluorescence microscopy	●		●		●		●	
Spectroscopic ellipsometry	(●)			(●)		●	(●)	●

electrical transport in the device and power generation during illumination. The most detailed source of information is the measurement of *IV*-curves as a function of time. From the evolution of the *IV*-curves information on J_{sc}, V_{oc}, FF, PCE, R_{sh}, R_s can be extracted and the general shape of the curve can be used to follow the degradation of the device performance. IPCE (or EQE) can in principle also be employed to follow the degradation process, but this has not been reported yet perhaps because a monitoring of J_{sc} essentially gives the same information albeit not in the same units and not specific to a particular wavelength.

4.1.1. Simple lifetime measurements

The maximum short circuit current, open circuit voltage, FF or power conversion efficiency (J_{sc}, V_{oc}, FF and PCE) is measured as a function of time. Of these parameters, the most useful ones are J_{sc} and PCE as they relate directly to device operation and reflect best how the device degrades. The V_{oc} also degrade as a function of device lifetime but not always in as straightforward a manner since it is not linked to the machinery of the cell in the same way as the J_{sc} and PCE that both reflect the ability of the device to convert photons into electrons or energy. By plotting a curve of the chosen parameter as a function of time a picture of the degradation is obtained. The shape of the curve may take many forms depending on what mechanisms or combination of mechanisms that are preponderant. The curves may follow a linear decay, an exponential decay or a combination. Often a period of device improvement is observed during the first part of the device life which can be due to annealing phenomena that lead to device improvement at a greater rate than device degradation initially. Alas, the degradation is inevitable and always takes over at some point.

The purpose of measuring the lifetime of a device through a decay curve has several purposes. Firstly, it establishes qualitatively whether the particular device is stable and how it degrades. Secondly and more importantly, it should allow for the comparison with devices prepared from different materials and thus ideally provide a method for improving polymer solar cell stability through design of materials, devices and fabrication methods. Even though this procedure is empirical it is in the absence of detailed understanding and knowledge of the degradation mechanisms the best approach. Thirdly, when comparing the device performance in terms of stability and degradation some suitable measure of stability needs to be chosen. There is currently no consensus on how to define stability and lifetime. So far the choice has in part been ruled by the degradation response of the device. For instance devices that can be fitted by an exponential function easily give access to the half-life as a parameter that can be obtained by fitting the entire curve and thus reflect accurately some measure of the stability or duration of operation. In the case of a linear response a linear fit is possible. There is then the problem of how to deal with devices that exhibit an improvement during the first phase of operation. Fourthly, some devices exhibit a constant degradation over a large part of the lifetime curve but the rate of degradation suddenly increases rapidly towards the end of the device life making projections of operational stability difficult based on the decay profile at the beginning of the device life. Finally, there is an issue of performance as one device type may be highly efficient but relatively short lived and another one may be less performing but very stable in operation. A comparison of two such technologies may be difficult even though they may both serve well in particular applications. Another measure in such a case is thus the integral of the J_{sc} curve or PCE curve over the entire service life giving the total charge or the total energy the particular device technology can produce during its operational lifetime. While it would be desirable to have a unique measure of the performance of a device technology in terms of stability this is difficult and could do injustice to some technologies and give unreasonable favor to others. It is therefore proposed that a series of considerations are made when wishing to compare lifetimes and stability performance of materials and device technologies. It is thus not reasonable to assume that a single fundamental parameter of degradation can be extracted and used to compare different devices. Rather, it is proposed that the stability and degradation is characterized according to a standard that then enable the unsuspecting reader to judge when and where a particular technology may be applied commercially combined with other factors. For instance, a short-lived high-yielding device type may be useful for one application whereas a low yielding but long-lived one may be useful in another type of application.

4.1.2. A standardized procedure

Presently, it may be difficult to compare results from different groups since there is no standardized lifetime test. Operational lifetimes have been measured in light, under different incident light intensities, with varying spectra (i.e. AM1.5G or unspecified), under continuous or intermittent illumination, in the dark, encapsulated, in inert atmosphere, in air, outside under real conditions, at different temperatures, at specified or unspecified levels of humidity, the conditions between measurements are usually not stated, are the devices kept in the dark or under illumination, under short or open circuit or under some bias voltage. All these aspects are making quantitative comparison virtually impossible and are complicated further by the fact that experimenters often have an interest in showing their data in the best possible way. To conclude, a standardized method of reporting data would not only be useful but is with all due likelihood an absolute requirement for further development of the field. It is perhaps premature to fully define such a standardized method in this review. A discussion of what such a standardized method should entail however serves the purpose of this review well and is given in the following. Further, full

compliance between the results obtained in different laboratories cannot be anticipated until complete instrumental packages are available commercially. The parameters that should be specified and addressed in the measurements are most easily listed along with how to deal with parameters that are not addressed in a given measurement:

- Light:
  - Source (solar simulator, halogen lamp, tungsten, laser source, real sun).
  - Intensity and intensity measurement (bolometric, silicon diode).
  - Spectrum and filters (AM1.5G, AM1.5D, spectrum analyzer).
  - Conditions (continuous, intermittent, intensity variation, dark storage).
- Electrical measurement:
  - Source measure unit and connection to the cell.
  - Conditions (IV-curves, J_{sc}, V_{oc}, conditions between measurements).
  - Number of measurement points, step speed and direction.
  - Total charge and total energy generated by the cell.
- Temperature:
  - Measurement (surface, substrate, surroundings).
  - Heating/cooling means (air circulation, solid contact heat transfer).
- Atmosphere:
  - Ambient, vacuum, inert, glovebox (ppm levels of O_2 and H_2O).
  - Humidity (humidity level, humidity control).
- Device conditions:
  - Solid substrate, flexible substrate, encapsulation, active area.
  - Electrical contacts (point contact, epoxy glue).
- Field testing:
  - Outdoor–indoor, day/night cycles.
  - Weather conditions.

This list should be considered when reporting data and while this is not expected that all points are addressed their consideration will make it easier for someone examining the data to evaluate the results.

4.1.3. Practical approach to reporting the operational lifetime

The definition of operational lifetime is in traditional engineering terms given as the period of time that elapses between the initial performance and the point where 80% of the initial performance has been reached. This approach is advised when considerations of application are made but the many different lifetime curves that may be observed should be borne in mind and it is advised to make measurements of the complete lifetime curve that will enable an applications engineer to evaluate if a given material technology has a stable or flat degradation regime that can enable application in spite of for instance a fast initial decay. For now the best that can be done is to report as much detail as possible and as carefully as possible.

4.1.4. IV curve measurements (diode characteristics)

The diode characteristics are obtained by measuring the current generated from the device while applying a source voltage over a range of values. The current obtained at zero applied voltage is the short circuit current (J_{sc}) and the voltage at which the current becomes zero is the open circuit voltage (V_{oc}). The product of these two parameters gives the theoretical maximum power of the device. In practice, the actual maximum power (P_{max}) generated is substantially smaller and the ratio between them gives the FF (Eq. (3)). The power conversion efficiency (η) is calculated using Eq. (4):

$$FF = \frac{I_{max} \times V_{max}}{I_{sc} \times V_{oc}}, \tag{3}$$

$$\eta = FF \frac{V_{oc} \times I_{sc}}{P_{in}}. \tag{4}$$

The diode characteristics can be modeled using the concept of the equivalent circuit to extract more parameters such as the series and parallel resistances of the device. The *IV* curve of an organic solar cell can however change dramatically as it decays. Glatthaar et al. [108,109] have shown that an inverted region in the *IV* curve (leading to a decrease in the FF) of the device could be ascribed to corrosion at the alumina interface as described in Section 2.3. This effect has also been observed to appear gradually during long-term measurements [50]. It is therefore useful to measure the whole diode characteristics at regular intervals instead of just a simple parameter such as the short circuit current. Padinger et al. [58] used this procedure to measure the degradation of MDMO-PPV/PCBM solar cells, in inert atmosphere, under illumination and in the dark. The fastest decay was observed for illuminated cells heated to 67 °C. Only the ratio of current to initial current versus time was reported however.

4.2. Methods providing information from non-specific locations in the device

While the half-life measurements and the *IV* curve measurements provide useful information on the photovoltaic properties other methods provide information (directly or indirectly) on either morphology or chemistry (or in some cases a combination of both). This group of techniques can be divided into two: (i) techniques that provide either morphological and/or chemical information from specific spatial locations in the device, and (ii) techniques that provide information from e.g. all layers and typically averaged over a large area perpendicular to the thickness of the device. Examples of the latter are given in the following with specific emphasis on the applicability with regard to studying OPV degradation. Most of the

spectroscopic techniques give results averaged over the whole device, such as the UV–vis and IR spectra though they can be adapted to give crude but useful two-dimensional (2D) information.

4.2.1. Impedance spectroscopy

Impedance or dielectric spectroscopy measures the dielectric properties of a material as a function of frequency. For a polymer solar cell, the results can be interpreted in terms of the equivalent circuit with a resistive/capacitive (RC) element. Usually, impedance spectra are plotted as the real part of the impedance versus the imaginary part. An RC element is seen as a semicircle from which the capacitance can be derived. The technique has been used to monitor the progress of the annealing process [109]. During degradation an inverted region in the diode characteristics have been observed that has been explained using impedance spectroscopy as the formation of a dielectric layer at the active layer/alumina interface possibly aluminum oxide as described in Section 2.6. Meltzer et al. have investigated the C_{60}/metal interface and concluded that the results could be explained by the formation of a depletion layer with n-doping of the C_{60} layer [97]. Pradhan and Pal studied photovoltaics composed of organic molecules of Rose Bengal and copper(-II)phthalocyanine and correlated the real part of the permittivity (ε') with the short circuit current [147].

4.2.2. UV–vis spectroscopy

Photo-oxidation of polymers used in organic solar cells are also called photobleaching because the process leads to loss in conjugation destroying the chromophores responsible for the color. The rate of singlet oxygen degradation of a PPV polymer and some substituted oligomers were investigated using UV–vis spectroscopy by Dam et al. [53] (see also Section 2.3). A plot of the linear correlation between the natural logarithm to the relative absorption ($\ln(A_t/A_0)$) and the photolysis time gave the rate constants (k_{deg}).

Kroon et al. [148] used the so-called light beam-induced current measurements (LBIC) to obtain 2-D maps of the polymer solar cell photoelectric response over time. In this technique, the cell is scanned with a light beam (xenon lamp source, 0.5 mm diameter) while the short circuit current (I_{sc}) is measured. The devices investigated were the MDMO-PPV:PCBM type with an initial efficiency (η) of 2.55%. Initially, the LBIC images showed that the response of the device was uniform over the active area and then degraded substantially over the 457 h test period.

Jeranko et al. [128] have used a similar type of laser-induced photocurrent efficiency mapping of MDMO-PPV/PCBM solar cells as they degraded over time. Most cells gave rather homogeneous images from the start that deteriorated especially at the edges. This effect could also be demonstrated clearly in a cross-sectional scan. After 2 weeks of degradation, the area that was still active had become very inhomogeneous and later developed into small islands after 2 months of dark storage. In a few instances, some areas at the right rim of the cells were up to three times more efficient than the rest of the solar cell. This believed to be due to special conditions during deposition of the aluminum layer and the conclusion was that the nature of the aluminum/polymer interface played a key role in the electron and hole transfer. It was suggested that this imaging technique might be useful in a combinatorial approach to track down variations across the device.

4.2.3. Near-field scanning optical microscopy (NSOM)

McNeill et al. used a modified NSOM technique called near-field scanning photocurrent microscopy (NSPM) to correlate morphology with current generation in polymer solar cells [149]. In this instrument light from a 409 nm laser illuminate the device through a fiber optic AFM-type tip that is scanned over the sample while the current response is monitored. Both normal AFM images and NSPM images can be taken at the same time allowing the direct comparison between the morphology and current response. No conclusions on how the device morphology affects the efficiency or degradation of polymer solar cells were made. This was only a demonstration of the possibilities of the technique. It has an obvious interest however, since it is one of a few methods that can characterize the solar cell performance at the nanometer level.

4.2.4. Infrared spectroscopy

Infrared spectroscopical techniques probe the local chemistry and can be used study the time dependant evolution of intensity of signals from discrete functional groups in polymers. Either IRAS (IRAS spectroscopy) or FTIR to investigate the degradation of PPV polymers in solar cells has been described in Section 2.2. These studies show a decrease in vinylene bond signals and an increase in carbonyl group signals expected in the oxidative degradation of this type of polymers [54,56,57].

4.2.5. X-ray reflectometry

Energy dispersive X-ray reflectometry has been used to study the time-dependant degradation of polymer solar cells based on MDMO-PPV/PCBM by Paci et al. [110,111]. The technique measures the reflected intensity of X-rays and probes the thickness, roughness and electron density of the layer structure of thin-film devices. Paci et al. used a white incident X-ray beam produced by a standard 2 kW tungsten anode X-ray tube and detected by a solid-state germanium detector. Cells composed of the structure: glass/ITO/PEDOT/MDMO-PPV:PCBM/Al or glass/ITO/MDMO-PPV:PCBM/LiF/Al were studied. The results showed oscillations in the reflected intensity that were interpreted as due to the aluminum electrode layer. The cells were investigated both under illumination and in the dark and a significant thickening of the layer was observed. Two possible explanations were offered. The first was that a reaction occurred at the aluminum polymer interface with the formation of an aluminum oxide layer. The second explanation was that indium atoms from the ITO layer diffused into

the organic layer. Independent results employing synchrotron radiation as the source of X-rays for the reflectometry experiment have confirmed that changes take place but also show that the surface roughness of the evaporated aluminum (~10 nm) is so large that X-ray reflection features are probably not observed from this layer [112].

4.3. Methods providing information from more or less specific locations in the device

The methods described in Section 4.2 provide spatially non-specific information, i.e. typically averaged information from either the entire device or from localized areas on the device surface but with the information averaged from all the device layers. Furthermore, some of the techniques can only be used on the individual materials prior to incorporation into the device, i.e. not directly on the OPV device.

From a degradation point of view, it is very useful to be able to describe the in-plane and/or in-depth distribution of morphology and/or chemistry. The applicability of the available techniques varies. Techniques such as TOF-SIMS and XPS are cable of performing surface sensitive imaging and depth profiling and are thus versatile techniques. Other techniques are entirely imaging techniques with varying lateral resolutions, e.g. AFM, SEM, interference microscopy and fluorescence microscopy. Often a suite of imaging techniques is used to obtain complementary information. Imaging techniques cannot be used directly on the OPV device (except on the surface of the outer electrode). Scattering techniques such as RBS and spectroscopic ellipsometry are unique in the sense that they can provide information from specific layers in the device without gaining access by physical means. In order to employ the pure imaging techniques and benefit from the complementary information, it is necessary to gain access to the various layers/interfaces of the device.

4.3.1. Device accessibility

Ideally each layer in the device should be selectively removed. However, this is not always possible and there is always the risk of modifying the exposed surfaces/interfaces. Various processes can interfere when exposing the surfaces/interfaces, such as reaction of exposed organic material with oxygen and water (if handled in ambient air). Another problematic phenomenon is surface segregation, i.e. once a layer has been removed it could induce surface segregation of species from at least the bulk layer material. These possible phenomena should be considered when interpreting the subsequent analysis data.

The procedure of gaining access to the device by stepwise removal of the layers is schematically described in Fig. 18. The shown device has the composition Al/C_{60}/C_{12}-PPV/PEDOT:PSS/ITO. The procedure will of course depend on the composition. The Al electrode can be removed from the intact device by carefully applying a piece of adhesive tape on the active area, which is then pulled off very quickly exposing the Al/C_{60} interface for surface analysis. The C_{60} layer is removed by dipping a cotton swap in chloroform, and gently sweeping it across the exposed surface. In this case, the C_{12}-PPV is also removed. Since both C_{60} and C_{12}-PPV are soluble in the same solvents it is not possible to selectively remove each layer. The exposed PEDOT:PSS surface can now undergo surface characterization. The PEDOT:PSS layer is not soluble in chloroform but in water, so the chloroform procedure is simply repeated using (ultrapure) water instead, which exposes the ITO surface for further surface analysis.

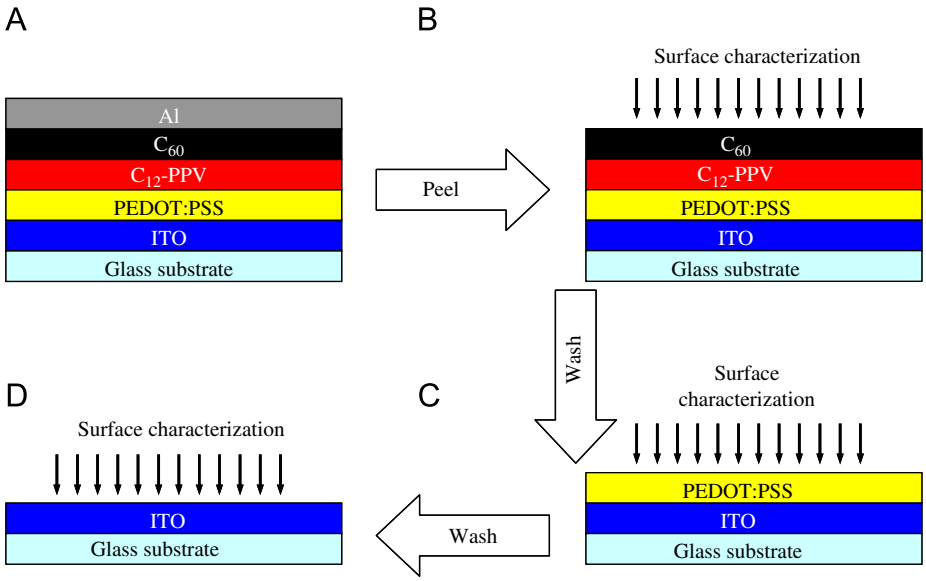

Fig. 18. Schematic showing the various steps involved in getting access to the various layers/interfaces of a device composed of Al/C_{60}/C_{12}-PPV/PEDOT:PSS/ITO: (A) The intact organic solar cell device. (B) The outcome of peeling off the Al electrode using adhesive tape. (C) The outcome of having washed off C_{60} and C_{12}-PPV using chloroform. (D) The outcome of having washed off the PEDOT:PSS using water. C_{12} corresponds to dodecyl.

4.3.2. Time-of-flight-secondary ion mass spectrometry

The versatile nature of TOF-SIMS has proven to be valuable when studying degradation mechanisms in OPVs. The probe depth is only 1–2 nm and the basic outcome is mass spectral information that contains an overwhelming amount of typically complex information. In particular for organic materials valuable information on the molecular structure can be obtained that enables monitoring of structural changes as a function of varied conditions, e.g. the effect of oxygen and/or water exposure on the molecular structure of the active material in an OPV during illumination or during storage in darkness. TOF-SIMS being a mass spectrometry-based technique makes it obvious and advantageous to employ isotopically labeled oxygen ($^{18}O_2$) or water ($H_2{}^{18}O$) in experiments dealing with oxidative degradation of OPVs and/or reaction with water.

4.3.2.1. Imaging. Besides obtaining a mass spectrum over and area of down to a few micrometers, TOF-SIMS can perform imaging as schematically illustrated in Fig. 19.

During analysis a mass spectrum is obtained from several points on the surface. Each point becomes a pixel in the resulting image, i.e. each pixel represents a mass spectrum. The intensity distribution of a mass spectral marker for a given species on the surface will then, via a color intensity bar (gray scale in Fig. 19), provide an (digital) ion intensity image of that species over the analyzed area, i.e. visualize the in-plane distribution of for example an oxidation product in an organic interface in the OPV. Different imaging techniques typically vary in probe depth, area coverage, lateral resolution (image resolution) and the type of information acquired. TOF-SIMS has, as mentioned earlier, a probe depth of 1–2 nm, area coverage from a few square micrometers to ~100 cm^2, a lateral resolution down to ~50 nm, and provides chemical information via mass spectral data.

Fig. 20 shows the result of imaging the accessible interfaces in an OPV device composed of Al/C_{60}/C_{12}-PPV/PEDOT:PSS/ITO. The device was illuminated (1000 W m^{-2}, AM1.5) in an $^{18}O_2/N_2$ atmosphere (1 atm) for 45 h and was subsequently imaged using TOF-SIMS. By monitoring the $^{18}O^-/^{16}O^-$ intensity ratio over the analyzed area, it becomes possible to visualize the ^{18}O incorporation that occurred during illumination (if incorporation did occur the ratio should exceed the natural ratio of 0.2%). The observed circular oriented incorporation in the lateral plane led to the conclusion that this type of incorporation is a consequence of microscopic holes in the Al electrode. $^{18}O_2$ diffuses vertically through the holes and expands in all lateral directions reacting with C_{60}, where after the ^{18}O becomes fixed in degradation products. The fact that incorporation is observed at all analyzed interfaces suggests that oxygen diffuses through the outer Al electrode and continues through all the other layers and ends up incorporated in the ITO electrode. Until these results, it was not known that oxygen diffuses through the entire device to the counter electrode.

4.3.2.2. Depth profiling. If the imaging analysis is complemented by a sputter process depth profiling becomes possible. Whereas TOF-SIMS imaging is used to visualize in-plane distribution of chemistry TOF-SIMS depth profiling is used to visualize in-depth distribution of chemistry. The process is schematically shown in Fig. 21. Switching between a sputter process (digging a hole in the surface) and imaging enables monitoring of chemistry as a function of depth, i.e. enables depth profiling. Since depth profiling is actually imaging as a function of depth, it is in fact 3D information that is acquired. The often unknown sputter rate varies for different materials (e.g. when going through the layers in an OPV device), so the actual depth is not well defined. Complementary techniques are typically used to determine the film thickness.

Not only oxygen is observed to diffuse through the outer electrode to the counter electrode, water has been shown to exhibit the same behavior. Fig. 22 shows depth profiles for a device with the composition Al/MEH-PPV:PCBM/PEDOT:PSS/ITO that was exposed to saturated $H_2{}^{18}O$ during illumination (1000 W m^{-2}, AM1.5). Water is, according to the depth profile, observed to be incorporated at least into the MEH-PPV:PCBM layer. However, an analysis equivalent to that shown in Fig. 22 confirmed that water also reaches the ITO and incorporates ^{18}O (the sputter process drastically reduces the sensitivity due to charge build-up).

Fig. 23 displays a depth profile of a device with the composition Al/C_{60}/P3CT/ITO, and shows depth profiles for Al^+ and In^+ that are mass spectral markers for the two counter electrodes aluminum and ITO. The two markers are detected through the entire device (disregarding the substrate). The explanation is found in the phenomenon called interlayer diffusion (not to be mistaken for interlayer

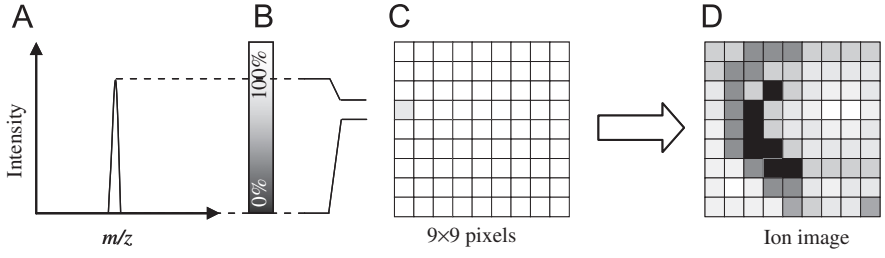

Fig. 19. Schematic of the process of creating an ion image from TOF-SIMS data.

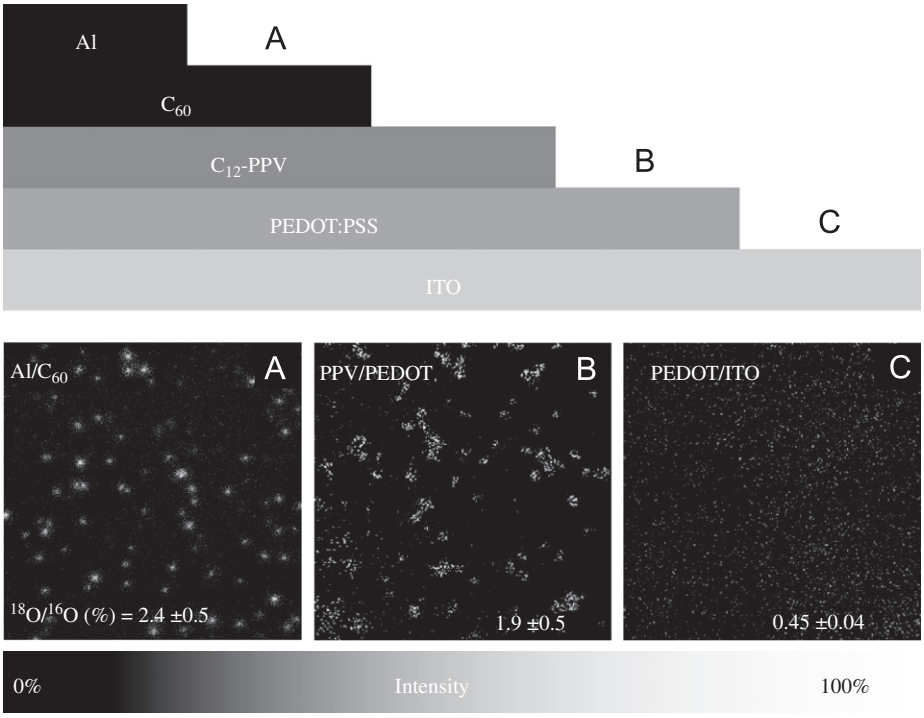

Fig. 20. TOF-SIMS images ($0.5 \times 0.5\,mm^2$) of three interfaces in an OPV device with the configuration Al/C_{60}/C_{12}-PPV/PEDOT:PSS/ITO. C_{12} corresponds to dodecyl. The images visualize the normalized lateral intensity distribution of the $^{18}O/^{16}O$ ratio. The $^{18}O/^{16}O$ ratio values in the lower right corners are averages of 10 measurements each covering $0.1 \times 0.1\,mm^2$ from various surface locations.

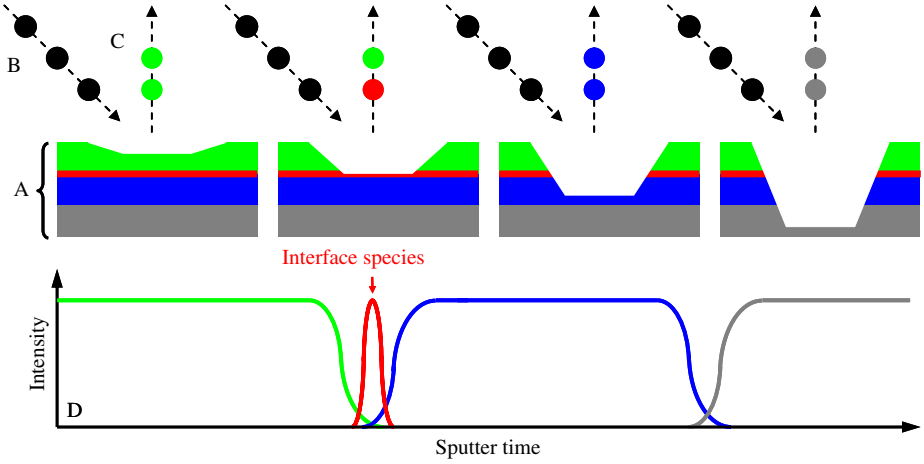

Fig. 21. Schematic of the process of performing a TOF-SIMS depth profile through a multilayer film (A). The surface is bombarded with sputter ions (B) that consequently removes material from the surface thus creating a hole. By switching between sputter ions (B) and analysis ions (primary ions) secondary ions (C) can be collected/detected as a function of the sputter time. A depth profile is constructed (D) by plotting the intensity of the secondary ions (specific ions from each layer) against the sputter time.

mixing). In this case, the electrode material is slowly dissolved in the other layers, i.e. electrode material is diffusing through the entire device and thus contributing to the overall degradation of the device.

TOF-SIMS has been used in numerous studies [45–51, 62,63,84,150–153] and also in the field of OLEDs [153,154].

4.3.3. *X-ray photoelectron spectroscopy*

XPS is very similar to TOF-SIMS in the sense that it has a probe depth of 5–10 nm, area coverage up to some square centimeters, a lateral resolution down to ~30 μm, and provides chemical information via measured core electron-binding energies. Furthermore, sputtering is also used in combination with this technique so depth profiling is also possible. The imaging capabilities and the sensitivity are inferior to that of TOF-SIMS. The strength of XPS, however, is the fact that is a quantitative technique that produces much less complex data compared with TOF-SIMS, which is relatively straightforward to interpret. XPS is an elemental analysis and provides valuable

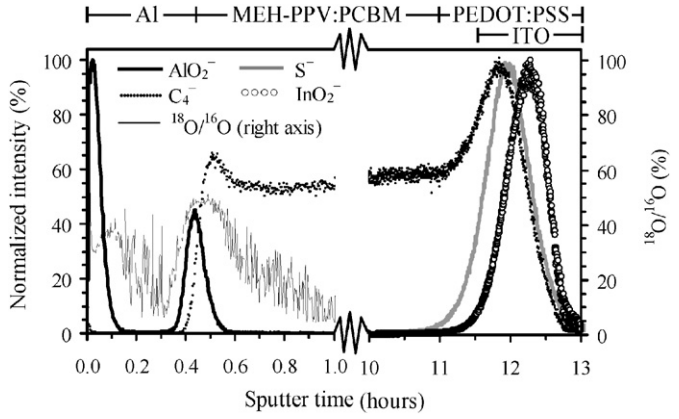

Fig. 22. TOF-SIMS depth profiles of an organic solar cell with the configuration Al/MEH-PPV:PCBM/PEDOT:PSS/ITO. AlO_2^- is a marker for aluminium oxide, C_4^- is a marker for MEH-PPV:PCBM and PEDOT:PSS, S^- is a marker for PEDOT:PSS, and InO_2^- is a marker for ITO.

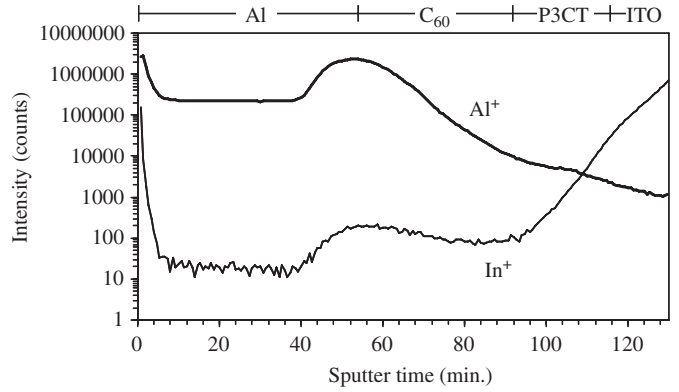

Fig. 23. TOF-SIMS depth profiles of an OPV device with the configuration Al/C_{60}/P3CT/ITO. P3CT corresponds to poly(3-carboxydithiophene).

(quantitative) information on the chemical state, which is especially useful with respect to carbon when studying OPV degradation. The depth profiling and imaging capabilities have not yet been exploited for the study of OPV degradation. Focus has been on averaged information on the chemical state. However, due to the complementary information XPS is often used in combination with TOF-SIMS.

4.3.4. Atomic force microscopy

AFM is an imaging technique that typically maps the surface with respect to surface topography (can, however, provide chemical contrast information if used in alternative modes). AFM can cover only a limited analysis area, but has an excellent lateral resolution (Ångstrøm range) and an excellent height resolution (Ångstrøm range), which makes it the obvious choice for the study of OPV degradation as a result of morphology changes on a nanoscale. However, the typical application for AFM with regard to OPVs has been to monitor and thus optimize the nanostructure of bulk heterojunction blend films in order to optimize the OPV efficiency.

AFM has been used to study the microscopic holes in the outer electrode of an OPV. It was found that each microscopic hole was centered in a surface protrusion. The microscopic holes were found to be the main entrance channels for oxygen and water and the protrusions was suggested to be a consequence of the resulting oxidation of the underlying organic material due to the formation of oxides (material build-up).

4.3.5. Scanning electron microscopy

SEM is an imaging technique and has become a standard tool for visualizing morphology in OPVs. The strength of the technique is the superior lateral resolution and the capability of analyzing a broad range of scales from nanometer range to millimeter range. The weakness is the lack of a depth scale.

Just as AFM the typical application for SEM with regard to OPVs has been to monitor and thus optimize nanostructures in order to optimize the OPV efficiency. SEM is, mainly because of the superior lateral resolution, cable of visualizing the bulk morphology of OPVs by imaging a cross-section of the device. This has, however, still not been utilized to study OPV degradation. Norrman et al. [47] used SEM in combination with AFM to, among other things, study the surface structure of the outer electrode of a device with the composition Al/C_{60}/C_{12}-PPV/PEDOT:PSS/ITO. The SEM image is shown in Fig. 24. The surface structure/morphology was observed to consist of aluminum grains with grain sizes ranging between ~10 and ~100 nm. The ability of oxygen and water to diffuse into the device through the outer electrode resulting in OPV degradation will depend on the electrode morphology, i.e. grain size, grain size distribution, hole sizes, hole density, etc. SEM is an excellent technique to monitor the outer electrode structure/morphology. However, work describing these phenomena with regard to degradation of OPVs is very scarce in the literature. Also,

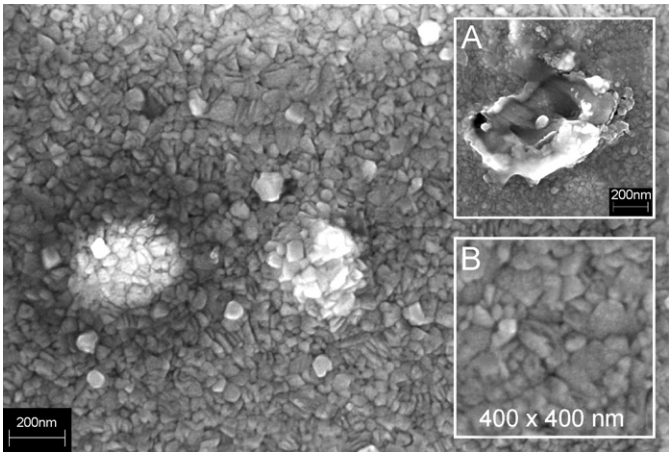

Fig. 24. SEM image ($2.3 \times 1.7\,\mu m^2$) of the outer electrode surface of a device with the composition Al/C_{60}/C_{12}-PPV/PEDOT:PSS/ITO.

SEM does hold the possibility for revealing chemical detail through energy dispersive X-ray analysis.

4.3.6. Interference microscopy

Interference microscopy is a spectroscopic imaging technique based on light, so the applicability is limited when it comes to transparent surfaces. The information obtained is surface topography, so it can be used in analogy with AFM and SEM, or rather as a complementary technique. The weakness of the technique is the inferior lateral resolution. The strength of interference microscopy is the excellent height resolution in the Ångström range combined with the ability to analyze large areas in the millimeter range fairly quickly (it is not a vacuum technique), so it is an excellent choice for screening for example electrode surfaces with respect to topography. Even though the method has a lot of potential, it has not been used much in the study of OPV degradation. Norrman et al. [47] used it to ascertain the protrusion and thus the hole density on the outer electrode of a device with the composition Al/C_{60}/C_{12}-PPV/PEDOT:PSS/ITO.

4.3.7. Fluorescence microscopy

Fluorescence microscopy is an imaging technique that visualizes possible fluorescence from the analyzed material, or in the case of more than one species being present visualizes contrast in emitted fluorescence. Norrman et al. [47] utilized this technique to monitor the extent of degradation caused by diffusion of oxygen and water into OPV devices with the composition Al/C_{60}/C_{12}-PPV/PEDOT:PSS/ITO. They obtained fluorescence images from two devices: (i) one that had been illuminated in air (Fig. 15c–d), (ii) and one that had been stored in darkness in air (Fig. 15a–b). The authors used the fact that the active material C_{12}-PPV is highly fluorescent but C_{60} and oxidized/degraded C_{60} are not (C_{60} actually quenches fluorescence). Based on the observation in Fig. 25, the authors concluded that storing the device in darkness in air causes only the C_{60} to be oxidized/degraded, and illumination in air causes both C_{60} and at least the sub-layer of C_{12}-PPV to be oxidized/degraded, i.e. the illumination appears, as expected, to accelerate the oxidation/degradation process.

4.3.8. Rutherford Backscattering (RBS)

RBS, nuclear reaction analysis, and elastic recoil detection analysis with incident MeV ions are powerful methods for the quantitative analysis of thin films and depth profiling of the near surface layers of solids. These are useful tools to investigate especially the electrode degradation mechanisms in solar cells.

4.4. Atmosphere studies (inert atmosphere, isotopically labeled oxygen and water)

As shown above, the degradation of polymer solar cells depends dramatically on the exposure to oxygen, water and

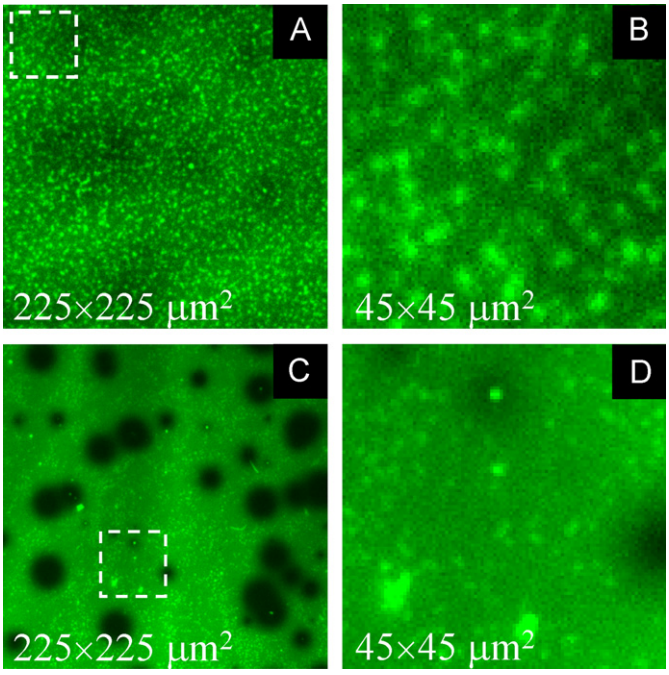

Fig. 25. Fluorescence microscopy images (excitation at 488 nm, emission at wavelengths >505 nm) obtained from OPVs with the composition Al/C_{60}/C_{12}-PPV/PEDOT:PSS/ITO after illumination in air (C and D) or after having been stored in darkness in air (A and B). The right images correspond to the areas indicated by white dashed squares in the left images.

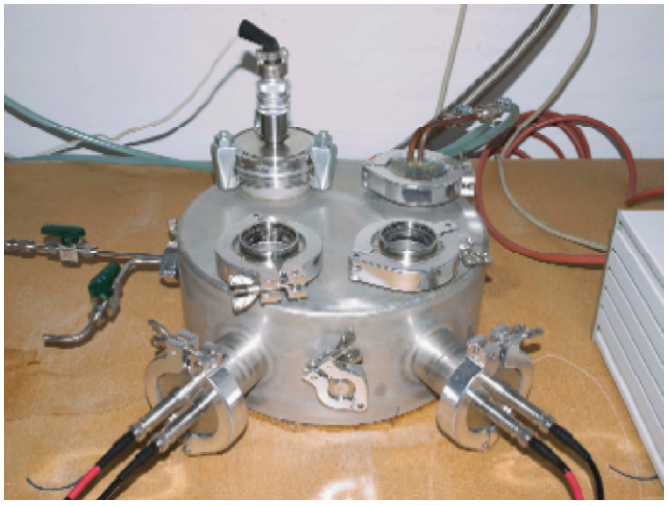

Fig. 26. Chamber for controlling the atmosphere and temperature during a lifetime test of solar cells.

on the temperature. It is therefore important to be able to control these parameters in a lifetime experiment. This can be done if the solar cell is contained in an airtight chamber with suitable connections to inert air supply, cooling or heating and electronic connections. A custom-built atmospheric chamber to investigate solar cells is shown in Fig. 26. The chamber is then placed under an artificial sun with light entering through two small circular windows directly above the solar cells under investigation [155].

With this device, it is also possible to introduce isotopic labeled gases like $^{18}O_2$ or $H_2{}^{18}O$ water vapor for studying the incorporation of oxygen in the polymer by mass spectrometric techniques (Fig. 26).

4.5. Accelerated testing

Device lifetime may be defined as the operational lifetime until the performance has fallen below a certain useful level. The decay may be an exponential function with one or more parts as shown in Eq. (1) and it is then appropriate to use the half-life or decay to 50% performance as a measure of the device lifetime. Presently, most polymer solar cell devices decay on the order of hours to months, which is feasible to measure directly. As polymer solar cells become more stable this is no longer possible. An accepted method is to use what is called accelerated testing was the half-life, which is artificially shortened by increasing the temperature or another parameter that influences the lifetime. The rationale is that the decay process, which may be chemical in nature follows an Arrhenius-type model where the rate of decay is determined by an exponential function:

$$k_{\mathrm{deg}} = A \exp\left(\frac{-E_{\mathrm{a}}}{RT}\right), \tag{5}$$

where E_{a} is the activation energy for the process in electron volt, T the temperature in Kelvin. A is a reaction dependant constant. If the decay follows this simple equation, it is evident that the rate of decay k_{deg} is very temperature dependent and can be calculated from Eq. (6):

$$K = \frac{k_{deg}(T_1)}{k_{deg}(T_2)} = \exp\left[\frac{E_{\mathrm{a}}}{k_{\mathrm{B}}}\left(\frac{1}{T_2} - \frac{1}{T_1}\right)\right]. \tag{6}$$

The acceleration factor K is the ratio between the rates of degradation (k_{deg}) at the two temperatures (T_1 and T_2) and k_{B} is the Boltzmann constant. The model is rather simplified. For instance, if more than one decay mechanism is operating they should all follow Eq. (5). The accelerated testing has been applied to MDMO-PPV/PCBM solar cells by Schuller et al. [134] where the acceleration factor K was measured in a temperature range of 40–105 °C. A roughly linear behavior of $\log(K)$ versus $1/T$ was observed with a more than ten-fold increase in the rate of degradation from 40 to 105 °C. This corresponds to an activation energy (E_{a}) of 300–350 meV. More complicated models that can take other factors than the temperature into account, like the Eyring model, was also considered.

De Bettignies et al. [135] did accelerated lifetime studies for the P3HT:PCBM system and found a decrease in performance measured as the short-circuit current (I_{sc}) of less than 15% after 200 h at 60 °C. Using the activation energy of 350 meV found in the previous study on MDMO-PPV/PCBM by Schuller at al., an acceleration factor of 4.45 was calculated. The 15% decrease in 200 h would thus correspond to 1000 h at 25 °C. The use of accelerated testing is however not simple as demonstrated by Gevorgyan et al. [155] where it was found that the acceleration factor may change during the lifetime and temperature independent processes may take place. Accelerated testing is probably the only realistic method when OPVs become more stable, but it must also be realized that it may not in all cases reflect how and how fast devices will degrade under normal working conditions. Two degradation processes could for instances have widely different Arrhenius activation energies with correspondingly different acceleration factors. As an example, take UV light degradation where light of 400 nm has an energy of 3 eV which is a lot of energy compared with the ordinary temperature scale where operation is at or around room temperature. Heating the sample by an extra 50–60 °C would probably not affect such a process much. Degradation by diffusion on the other hand depends on the diffusion coefficient of the chemical species responsible for the decay. This diffusion coefficient is temperature dependent according to an Arhenius-type exponential equation. So in theory, at low temperature, the UV degradation processes may dominate, while the diffusion process would take over at higher temperatures. Accelerated testing would lump both processes together giving a false picture of the temperature dependence of the stability of the device. Further, there are several processes leading to device degradation and unless they are all accounted for it is very difficult to establish why devices degrade under a given set of conditions.

4.6. Outdoor testing

Polymer solar cells have almost exclusively been tested in a controlled laboratory environment. A few reports on real-life outdoor testing have appeared however. A very preliminary result on module efficiency of ITO/MEH-PPV/PCBM/Al cells printed on a flexible was subjected to a Danish winter with an intermittent snow storm (Fig. 27). A rapid decay over a 12-day period was observed and mostly ascribed to the lack of encapsulation since the light intensity during daytime was limited. More rigorous tests of encapsulated single cells were carried out in the Negev desert by Katz et al. [129,130]. Over a 32-day period [130], three different solar cells with different active layers of either MEH-PPV, P3HT or P3CT in bulk heterojunction and bilayer heterojunction geometries with PCBM. All three cells were encapsulated with a heavy aluminum back plate, a glass front plate sealed with glass-filled thermosetting epoxy glue [44].

The cells were exposed to sunlight (and high temperatures up to 45 °C) in the air during daytime and stored under nitrogen at night. The output power of the cells was adjusted to the standard irradiance of 1000 W m^{-2}. As expected, the MEH-PPV cell degraded fast in some 60–70 h of cumulative sunlight. The P3CT cells survived the longest with an almost unchanged FF. The performance dropped by a factor of ca. two over some 160 h of cumulative sunlight. A curious restorative behavior was found for the

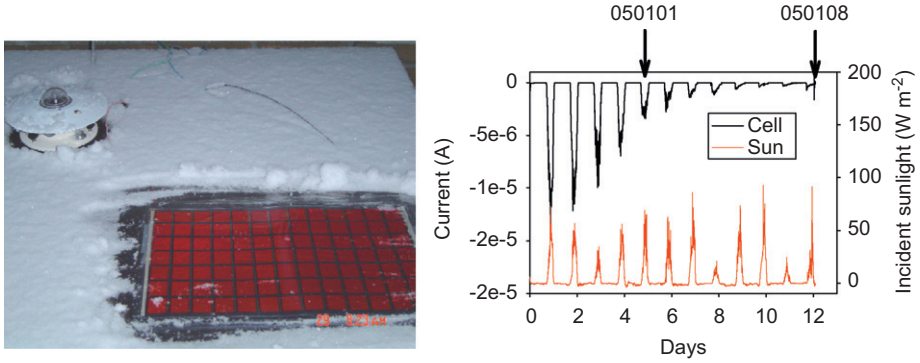

Fig. 27. Outdoor testing of a large encapsulated module during a Danish winter. The already low-efficiency cells died quickly during a few days exposure (black line) the light intensity is measured with a pyranometer is also shown (red line).

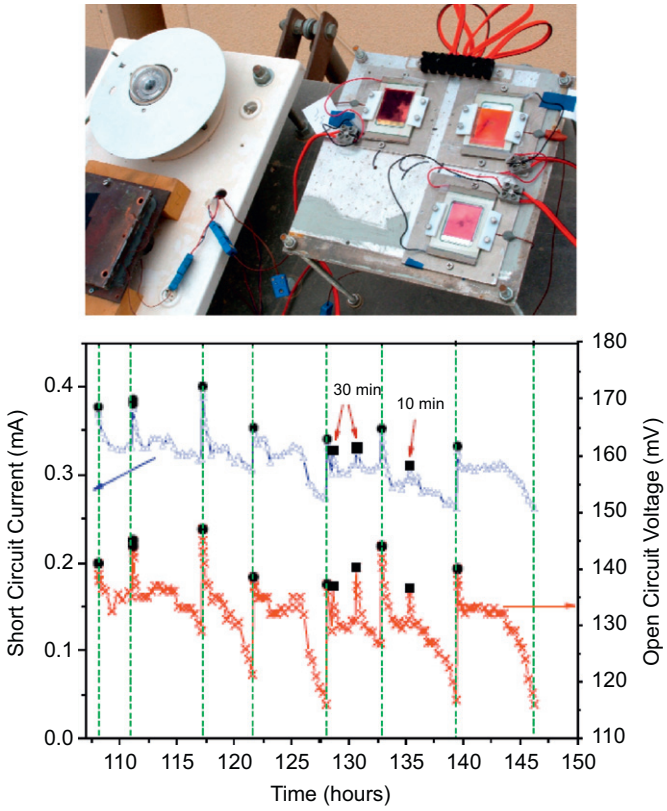

Fig. 28. Outdoor testing of polymer solar cells in the Negev desert of Israel.

cells made with P3HT and P3CT. Both short circuit current and open circuit voltage dropped during daytime, but recovered almost fully during nighttime. The cells were usually kept in nitrogen at night and the effect of the atmosphere and this restorative behavior was therefore tested by storing them in the air instead. A similar behavior was observed and can therefore not be due to the nitrogen. It was concluded that some reversible photochemical degradation must be at work perhaps a slow removal of photo-induced charge traps. Because of this effect, it is not clear how one can compare these outdoor tests with accelerated laboratory tests and tests with no dark recovery periods (Fig. 28).

5. Encapsulation techniques

5.1. Encapsulation membranes

The polymer solar cells sensitivity towards oxygen and moisture makes it imperative to protect them with some sort of encapsulation. Presently, glass is used as the transparent substrate for the devices and it is of course impermeable. The thin metal electrode evaporated on top is however, porous enough to allow gas transport. Flexible substrates like poly(ethylene terephthalate) (PET) or poly(ethylene naphthalate) (PEN) increase the problems due to their fast transport of oxygen and water.

The rate of transport across membranes is expressed in the oxygen transmission rate (OTR) and the water vapor transmission rate (WVTR). Rather stringent requirements for these parameters are generally accepted for OLEDs and probably apply to organic solar cells as well. Upper limits of ca. $10^{-3}\,cm^3\,m^{-2}\,day^{-1}\,atm^{-1}$ for OTR and $10^{-4}\,g\,m^{-2}\,day^{-1}$ for WVTR have been proposed for organic solar cells [131–133] (Fig. 29).

Commercial PET and PEN polymer films have much higher rates of transport. Certain kinds of food and pharmaceutical packaging also require better barrier properties to avoid oxidation that has led to the development of improved polymer films with in-built barrier layers. These layers may be inorganic oxides deposited by plasma-enhanced chemical vapor deposition reaching permeation levels 1000 times lower than for the native polymer films. Multilayered barrier films consisting of alternating inorganic SiO_x and polymer PEN substrates were used to greatly increase the lifetime of MDMO-PPV/PCBM-type solar cells. Shelf lifetimes of more than 6000 h were reported [131–133]. A more rigid encapsulation technique has been investigated by F.C. Krebs, where the device is sandwiched between a thick aluminum back plate and a front glass plate and sealed with thermosetting epoxy glue [44]. Such an encapsulation is probably almost totally

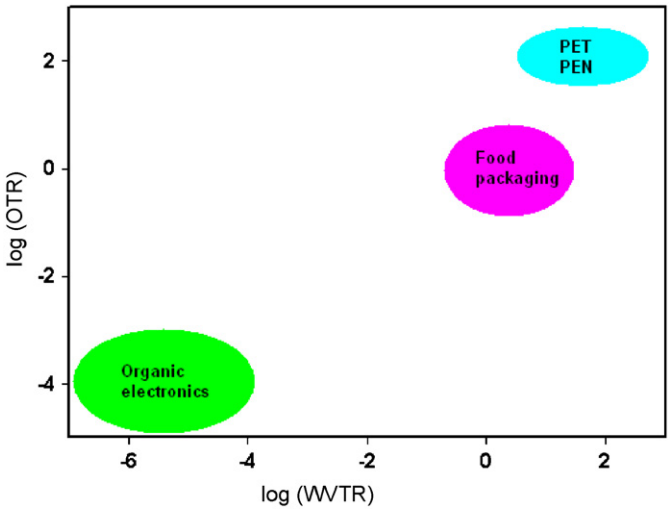

Fig. 29. For commercial polymers (PEN and PET) and the limits required for food packaging and organic electronics, respectively. Adapted from Dennler et al. [131–133].

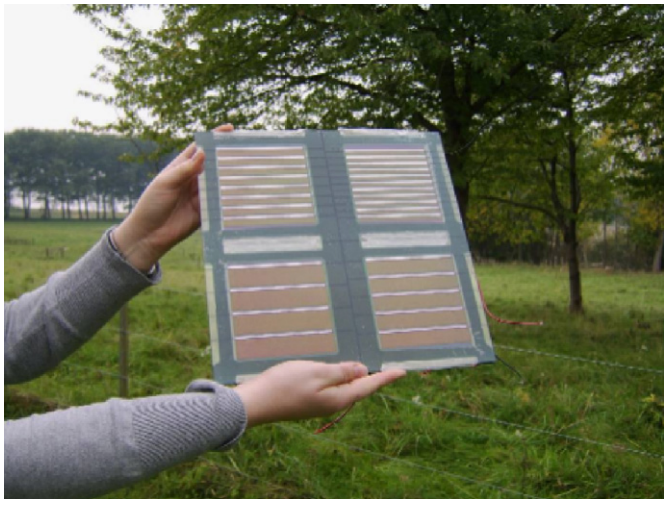

Fig. 30. Rigidly encapsulated array of cells with a thick alumina back plate.

impermeable to both oxygen and moisture and it allowed more than 1-year operation of a large area P3HT/PCBM bulk heterojunction. The cell had a modest efficiency of 0.48% (η) and a year latter this had dropped to 0.31% corresponding to a 25% loss of efficiency. This type of encapsulation is of course not flexible, but may be a convenient technique for laboratory use (Fig. 30).

Other encapsulation techniques tested include parylene coating in combination with aluminum oxide [156] and cover lids with getter materials [157].

6. Conclusions

The field of polymer solar cells undergoes a rapid development where most of the research effort has been placed on developing devices with an improved efficiency. An equally important area that has received less attention is to extend the rather poor stability seen in the initial devices. Some progress has been made as detailed above. Polymer solar cells are complicated multilayer structures where each component may fail for different reasons and layers may even interact chemically and physically in ways that may cause degradation. Understanding is far from complete, but some main contributors to the degradation mechanisms have been pin pointed. Oxygen from the atmosphere will oxidize the organic layer, especially when the device is illuminated. This may seem to be a paradox: solar cells that degrade when exposed to light! Fortunately, newer materials such as P3HT and better P3CT are less prone to this degradation pathway. Most polymer solar cells today rely on the formation of bulk heterojunction, an interpenetrating network of donor and acceptor material. The micro phase-separation, developed through the process of annealing, to get the morphology/structure is very important to obtain efficient devices. Unfortunately, this "right" structure/morphology is not at the thermodynamic equilibrium, so the further structural changes can occur, especially when devices are heated. Other types of polymer solar cells employ inorganic oxides such as titanium oxide as electron accepting materials. It has been shown that under UV irradiation nanocrystalline titania will catalyze the photodegradation of polymers. Other oxides may be reversibly depleted of oxygen under illumination. These processes may compete with the charge separation in photovoltaic operation. Alumina, which is the most commonly used metal electrode, is also set up to react with oxygen and water and perhaps even with the polymer material due to its low work function. The transparent electrode, which is commonly ITO, has been shown to be less than ideally stable also. Indium atoms escape and distribute themselves into the polymer layer. The PEDOT:PSS layer used to extract the positive carriers is hygroscopic in nature and may bind sufficient water to cause havoc later. It also seems to be a less characterized material where some material may crystallize to form point defects. Finally, the devices may fail due to mechanical instabilities leading to delamination. In all, a varied list of possible factors in degradation with varying degrees of impact on the device lifetime. More stable devices have already been made and progress in this research field is important for polymer solar cells to have a future as commercial devices.

References

[1] C.J. Brabec, N.S. Sariciftci, J.C. Hummelen, Adv. Funct. Mater. 11 (2001) 15.
[2] H. Spanggaard, F.C. Krebs, Sol. Energy Mater. Sol. Cells 83 (2004) 125.
[3] K.M. Coakley, M.D. McGehee, Chem. Mater. 16 (2004) 4533.
[4] H. Hoppe, N.S. Sariciftci, J. Mater. Res. 19 (2004) 1924.
[5] S. Günes, H. Neugebauer, N.S. Sariciftci, Chem. Rev. 107 (2007) 1324.
[6] C. Winder, N.S. Sariciftci, J. Mater. Chem. 14 (2004) 1077.

[7] E. Bundgaard, F.C. Krebs, Sol. Energy Mater. Sol. Cells 91 (2007) 954.
[8] B.P. Rand, J. Genoe, P. Heremans, J. Poortmans, Prog. Photovolt. Res. Appl. 15 (2007) 659.
[9] F.C. Krebs (Ed.), Special Issue: The development of organic and polymer photovoltaics, Sol. Energy Mater. Sol. Cells 83 (2–3) (2004).
[10] S.E. Shaheen, D.S. Ginley, G.E. Jabbour (Eds.), Special Issue: Organic-Based Photovoltaics, MRS Bull 30 (1) (2005).
[11] F.C. Krebs (Ed.), Special Issue: low band gap polymer materials for organic photovoltaics, Sol. Energy Mater. Sol. Cells 91 (11) (2007).
[12] M.T. Loyd, J.E. Anthony, C.G. Malliaras (Eds.), Special Issue: a real alternative. Materials and devices for cheap efficient solar power, Mater. Today 10 (11) (2007).
[13] J. Poortmans (Ed.), Special Issue. Prog. Photovolt., Res. Appl. 15 (8) (2007).
[14] S.E. Shaheen, D.S. Ginley, G.E. Jabbour, MRS Bull. 30 (2005) 10.
[15] R.A.J. Janssen, J.C. Hummelen, N.S. Sariciftci, MRS Bull. 30 (2005) 33.
[16] K.M. Coakley, Y. Liu, C. Goh, M.D. McGehee, MRS Bull. 30 (2005) 37.
[17] C.J. Brabec, J.A. Hauch, P. Schilinsky, C. Waldauf, MRS Bull. 30 (2005) 50.
[18] A.C. Mayer, S.R. Scully, B.E. Hardin, M.W. Rowell, M.D. McGehee, Mater. Today 10 (2007) 28.
[19] M.T. Lloyd, J.E. Anthony, G.G. Malliaras, Mater. Today 10 (2007) 34.
[20] J.Y. Kim, K. Lee, N.E. Coates, D. Moses, T.-Q. Nguyen, M. Dante, A.J. Heeger, Science 317 (2007) 222.
[21] G. Li, V. Shrotriya, J. Huang, Y. Yao, T. Moriarty, K. Emery, Y. Yang, Nat. Mater. 4 (2005) 864.
[22] W. Ma, C. Yang, X. Gong, K. Lee, A.J. Heeger, Adv. Funct. Mater. 15 (2005) 1617.
[23] S.R. Forrest, MRS Bull. 30 (2005) 28.
[24] L.J.A. Koster, V.D. Mihailetchi, P.W.M. Blom, Appl. Phys. Lett. 88 (2006) 093511.
[25] M.C. Scharber, D. Mühlbacher, M. Koppe, P. Denk, C. Waldauf, A.J. Heeger, C.J. Brabec, Adv. Mater. 18 (2006) 789.
[26] J. Gilot, M.M. Wienk, R.A.J. Janssen, Nat. Mater. 6 (2007) 704.
[27] (a) G. Dennler, Mater. Today 10 (2007) 56;
(b) G.P. Smestad, F.C. Krebs, C.M. Lampert, C.G. Granquist, K.L. Chopra, X. Mathew, H. Takakura, Sol. Energ. Mater. Sol. Cells 92 (2008) 371–373.
[28] C.J. Brabec, Sol. Energy Mater. Sol. Cells 83 (2004) 273.
[29] F.C. Krebs, Refocus 6 (2005) 38.
[30] G. Yu, C. Zhang, A.J. Heeger, Appl. Phys. Lett. 64 (1994) 1540.
[31] H. Hänsel, H. Zettl, G. Krausch, R. Kisselev, M. Thelakkat, H.W. Schmidt, Adv. Mater. 15 (2003) 2056.
[32] ASTM International, Standard Tables for Reference Solar Spectral Irradiances: Direct Normal and Hemispherical on 37° Tilted Surface, G 173-03, 2003. The data can be downloaded at; ⟨http://rredc.nrel.gov/solar/spectra/am1.5/⟩.
[33] ASTM International, Standard Specification for solar simulation for photovoltaic testing, E 927-05, 2005.
[34] IEC 904-9, Photovoltaic devices—Part 9: Solar simulator performance requirements, 1995, IEC 904-9:1995(E).
[35] (a) A. Moliton, J.-M. Nunzi, Polym. Int. 55 (2006) 583;
(b) S.E. Shaheen, Reliability physics symposium, 15–19 (2007) 248–252. (doi:10.1109/RELPHY.2007.369900).
[36] F.C. Krebs, J.E. Carlé, N. Cruys-Bagger, M. Andersen, M.R. Lilliedal, M.A. Hammond, S. Hvidt, Sol. Energy Mater. Sol. Cells 86 (2005) 499.
[37] C. Féry, B. Racine, D. Vaufrey, H. Doyeux, S. Cinà, Appl. Phys. Lett. 87 (2005) 213502.
[38] N. Chawdhury, A. Köhler, M.G. Harrison, D.H. Hwang, A.B. Holmes, R.H. Friend, Synth. Met. 102 (1999) 871.
[39] B.M. Henry, F. Dinelli, K.-Y. Zhao, C.R.M. Grovenor, O.V. Kolosov, G.A.D. Briggs, A.P. Roberts, R.S. Kumar, R.P. Howson, Thin Solid Films 355–356 (1999) 500.
[40] A.G. Erlat, B.M. Henry, J.J. Ingram, D.B. Mountain, A. McGuigan, R.P. Howson, C.R.M. Grovenor, G.A.D. Briggs, Y. Tsukahara, Thin Solid Films 388 (2001) 78.
[41] M. Yanaka, B.M. Henry, A.P. Roberts, C.R.M. Grovenor, G.A.D. Briggs, A.P. Sutton, T. Miyamoto, Y. Tsukahara, N. Takeda, R.J. Chater, Thin Solid Films 397 (2001) 176.
[42] A.P. Roberts, B.M. Henry, A.P. Sutton, C.R.M. Grovenor, G.A.D. Briggs, T. Miyamoto, M. Kano, Y. Tsukahara, M. Yanaka, J. Membr. Sci. 208 (2002) 75.
[43] A.G. Erlat, B.M. Henry, C.R.M. Grovenor, A.G.D. Briggs, R.J. Chater, Y. Tsukahara, J. Phys. Chem. B 108 (2004) 883.
[44] F.C. Krebs, Sol. Energy Mater. Sol. Cells 90 (2006) 3633.
[45] K. Norrman, F.C. Krebs, Surf. Interface Anal. 36 (2004) 1542.
[46] K. Norrman, F.C. Krebs, Sol. Energy Mater. Sol. Cells 90 (2006) 213.
[47] K. Norrman, N.B. Larsen, F.C. Krebs, Sol. Energy Mater. Sol. Cells 90 (2006) 2793.
[48] M. Lira-Cantu, K. Norrman, J.W. Andreasen, F.C. Krebs, Chem. Mater. 18 (2006) 5684.
[49] K. Norrman, F.C. Krebs, Proc. SPIE 5938 (59380D) (2005) 1.
[50] F.C. Krebs, K. Norrman, Prog. Photovol. Res. Appl. 15 (2007) 697.
[51] K. Norrman, J. Alstrup, M. Jørgensen, N.B. Larsen, M. Lira-Cantu, F.C. Krebs, Proc. SPIE 6334 (63340O) (2006).
[52] D.L. Rode, V.R. Gaddam, J.H. Yi, J. Appl. Phys. 102 (2007) 024303.
[53] R.D. Scurlock, B. Wang, P.R. Ogilby, J.R. Sheats, R.L. Clough, J. Am. Chem. Soc. 117 (1995) 10194.
[54] N. Dam, R.D. Scurlock, B. Wang, L. Ma, M. Sundahl, P.R. Ogilby, Chem. Mater. 11 (1999) 1302.
[55] B.H. Cumpston, K.F. Jensen, J. Appl. Polym. Sci. 69 (1998) 2451.
[56] R.F. Bianchi, D.T. Balogh, M. Tinani, R.M. Faria, E.A. Irene, J. Polym. Sci. Part B: Polym. Phys. 42 (2004) 1033.
[57] H. Neugebauer, C.J. Brabec, J.C. Hummelen, R.A.J. Janssen, N.S. Sariciftci, Synth. Met. 102 (1999) 1002.
[58] H. Neugebauer, C.J. Brabec, J.C. Hummelen, N.S. Sariciftci, Sol. Energy Mater. Sol. Cells 61 (2000) 35.
[59] F. Padinger, T. Fromherz, P. Denk, C.J. Brabec, J. Zettner, T. Hierl, N.S. Sariciftci, Synth. Met. 121 (2001) 1605.
[60] S. Chambon, A. Rivaton, J.-L. Gardette, M. Firon, Sol. Energy Mater. Sol. Cells 91 (2007) 394.
[61] S. Chambon, A. Rivaton, J.-L. Gardette, M. Firon, L. Lutzen, J. Pol. Sci. Part A: Pol. Chem. 45 (2007) 317.
[62] J. Alstrup, K. Norrman, M. Jørgensen, F.C. Krebs, Sol. Energy Mater. Sol. Cells 90 (2006) 2777.
[63] K. Norrman, J. Alstrup, M. Jørgensen, F.C. Krebs, Surf. Interface Anal. 38 (2006) 1302.
[64] M.S.A. Abdou, F.P. Orfino, Y. Son, S. Holdcroft, J. Am. Chem. Soc. 119 (1997) 4518.
[65] M.G. Matturro, R.P. Reynolds, R.V. Kastrup, C.F. Pictroski, J. Am. Chem. Soc. 108 (1986) 2775.
[66] L. Lüer, H.-J. Egelhaaf, D. Oelkrug, G. Cerullo, G. Lanzani, B.-H. Huisman, D. de Leeuw, Org. Electr. 5 (2004) 83.
[67] R. de Bettignies, J. Leroy, S. Chambon, M. Firon, C. Sentein, L. Sicot, L. Lutzen, Proc. SPIE 5464 (2004) 122.
[68] R. de Bettignies, J. Leroy, S. Chambon, M. Firon, C. Sentein, L. Sicot, L. Lutzen, Proc. SPIE 5520 (2004) 216.
[69] F.C. Krebs, R.B. Nyberg, M. Jørgensen, Chem. Mater. 16 (2004) 1313.
[70] K.T. Nielsen, K. Bechgaard, F.C. Krebs, Macromolecules 38 (2005) 658.
[71] K.T. Nielsen, K. Bechgaard, F.C. Krebs, Synthesis (2006) 1639.
[72] K.T. Nielsen, P. Harris, K. Bechgaard, F.C. Krebs, Acta Crystallogr. B 63 (2007) 151.
[73] M.M. Wienk, M.P. Struijk, R.A.J. Janssen, Chem. Phys. Lett. 422 (2006) 488.

[74] B.C. O'Regan, M. Grätzel, Nature 353 (1991) 737.
[75] L. Xiao-e, A.N.M. Green, S.A. Haque, A. Mills, J.R. Durrant, J. Photochem. J. Photobiol. A: Chem. 162 (2004) 253.
[76] A.M. Peiró, G. Doyle, A. Mills, J.R. Durrant, Adv. Mater. 17 (2005) 2365.
[77] A. Mills, G. Doyle, A.M. Peiró, J. Durrant, J. Photochem. J. Photobiol. A: Chem. 177 (2006) 328.
[78] A.M. Peiró, C. Colombo, G. Doyle, J. Nelson, A. Mills, J.R. Durant, J. Phys. Chem. B 110 (2006) 23255.
[79] P. Ravirajan, S.A. Haque, J.R. Durrant, D. Poplavskyy, D.D.C. Bradley, J. Nelson, J. Appl. Phys. 95 (2004) 1473.
[80] P. Ravirajan, S.A. Haque, D. Poplavskyy, J.R. Durrant, D.D.C. Bradley, J. Nelson, Thin Solid Films 451–452 (2004) 624.
[81] P. Ravirajan, D.D.C. Bradley, J. Nelson, S.A. Haque, J.R. Durrant, H.J.P. Smit, J.M. Kroon, Appl. Phys. Lett. 86 (2005) 143101.
[82] P. Ravirajan, S.A. Haque, J.R. Durrant, D.D.C. Bradley, J. Nelson, Adv. Funct. Mater. 15 (2005) 609.
[83] M. Lira-Cantu, F.C. Krebs, Sol. Energy Mater. Sol. Cells 90 (2006) 2076.
[84] M. Lira-Cantu, K. Norrman, J.W. Andreasen, N. Casan-Pastor, F.C. Krebs, J. Electrochem. Soc. 154 (2007) B508.
[85] W.J.E. Beek, M.M. Wienk, M. Kemerink, X. Yang, R.A.J. Janssen, J. Phys. Chem. B 109 (2005) 9505.
[86] D.C. Olson, J. Piris, R.T. Collins, S.E. Shaheen, D.S. Ginley, Thin Solid Films 496 (2006) 26.
[87] W.J.E. Beek, M.M. Wienk, R.A.J. Janssen, Adv. Funct. Mater. 16 (2006) 1112.
[88] H. Aziz, G. Xu, Synth. Met. 80 (1996) 7.
[89] H. Aziz, Z.D. Popovic, N.-X. Hu, A. Hor, G. Xu, Science 283 (1999) 1900.
[90] H. Aziz, Z.D. Popovic, Chem. Mater. 16 (2004) 4522.
[91] M. Lögdlund, J.L. Brédas, J. Chem. Phys. 101 (1994) 4357.
[92] M. Fahlman, D. Beljonne, M. Lögdlund, R.H. Friend, A.B. Holmes, J.L. Brédas, W.R. Salaneck, Chem. Phys. Lett. 214 (1993) 327.
[93] M. Fahlman, P. Bröms, D.A. dos Santos, S.C. Moratti, N. Johansson, K. Xing, R.H. Friend, A.B. Holmes, J.L. Brédas, W.R. Salaneck, J. Chem. Phys. 102 (1995) 8167.
[94] H. Antoniadis, B.R. Hsieh, M.A. Abkowitz, S.A. Jenekhe, M. Stolka, Synth. Met. 62 (1994) 265.
[95] S. Gamerith, C. Gadermaier, H.-G. Nothofer, U. Scherf, E.J.W. List, Proc. SPIE 5464 (2004) 104.
[96] S. Cros, M. Firon, S. Lenfant, P. Trouslard, L. Beck, Nucl. Inst. Meth. Phys. Res. B 251 (2006) 257.
[97] C. Melzer, V.V. Krasnikov, G. Hadziioannou, Appl. Phys. Lett. 82 (2003) 3101.
[98] J. Nishnaga, T. Aihara, H. Yamagata, Y. Horikoshi, J. Cryst. Growth 278 (2005) 633.
[99] M. Vogel, S. Doka, Ch. Breyer, M.Ch. Lux-Steiner, K. Fostiropoulos, Appl. Phys. Lett. 89 (2006) 163501.
[100] F. Li, H. Tang, J. Anderegg, J. Shinar, Appl. Phys. Lett. 70 (1997) 1233.
[101] S.T. Zhang, Y.C. Zhou, J.M. Zhao, Y.Q. Zhan, Z.J. Wang, Y. Wu, X.M. Ding, X.Y. Hou, Appl. Phys. Lett. 89 (2006) 043502.
[102] L.S. Hung, C.W. Tang, M.G. Mason, Appl. Phys. Lett. 70 (1997) 152.
[103] C.J. Brabec, S.E. Shaheen, C. Winder, N.S. Sariciftci, Appl. Phys. Lett. 80 (2002) 1288.
[104] W.J.H. van Gennip, J.K.J. van Duren, P.C. Thüne, R.A. Janssen, J.W. Niemantsverdriet, J. Chem. Phys. 117 (2002) 5031.
[105] N. Karst, J.C. Bernède, Phys. Stat. Sol. A 203 (2006) R70.
[106] F.C. Krebs, H. Spanggaard, Chem. Mater. 17 (2005) 5235.
[107] M. Bjerring, J.S. Nielsen, A. Siu, N. Chr. Nielsen, F.C. Krebs, Sol. Energy Mater. Sol. Cells 92 (2008) 782–794, this issue; doi:10.1016/j.solmat.2007.11.008.
[108] M. Glatthaar, M. Riede, N. Keegan, K. Sylvester-Hvid, B. Zimmermann, M. Niggemann, A. Hinsch, A. Gombert, Sol. Energy Mater. Sol. Cells 91 (2007) 390.
[109] M. Glatthaar, N. Mingirullim, B. Zimmermann, T. Ziegler, R. Kern, M. Niggemann, A. Hinsch, A. Gombert, Phys. Stat. Sol. A 202 (2005) R125.
[110] B. Paci, A. Generosi, V.R. Albertini, P. Perfetti, B. de Bettignies, M. Firon, J. Leroy, C. Sentein, Appl. Phys. Lett. 87 (2005) 194110.
[111] B. Paci, A. Generosi, V.R. Albertini, P. Perfetti, B. de Bettignies, M. Firon, J. Leroy, C. Sentein, Appl. Phys. Lett. 89 (2006) 043507.
[112] J.W. Andreasen, S. Gevorgyan, C.M. Schlepuetz, F.C. Krebs, Sol. Energy Mater. Sol. Cells 92 (2008) 803–808, this issue; doi:10.1016/j.solmat.2008.02.011.
[113] M.P. de Jong, L.J. van Ijzendoorn, M.J.A. de Voigt, Appl. Phys. Lett. 77 (2000) 2255.
[114] R. Pacios, A.J. Chatten, K. Kawano, J.R. Durrant, D.D.C. Bradley, J. Nelson, Adv. Funct. Mater. 16 (2006) 2117.
[115] K. Kawano, R. Pacios, D. Poplavskyy, J. Nelson, D.D.C. Bradley, J.R. Durrant, Sol. Energy Mater. Sol. Cells 90 (2006) 3520.
[116] J.S. Liu, E.N. Kadnikova, Y.X. Liu, M.D. McGehee, J.M.J. Fréchet, J. Am. Chem. Soc. 126 (2004) 9486.
[117] F.C. Krebs, Proc. SPIE 5938 (2005) 59380Y.
[118] X. Yang, J. Loos, S.C. Veenstra, W.J.H. Verhees, M.M. Wienk, J.M. Kroon, M.A.J. Michels, R.A.J. Janssen, Nano Letters 5 (2005) 579.
[119] F.C. Krebs, J. Alstrup, H. Spanggaard, K. Larsen, E. Kold, Sol. Energy Mater. Sol. Cells 83 (2004) 293.
[120] E. Bundgaard, F.C. Krebs, Pol. Bull. 55 (2005) 157.
[121] F.C. Krebs, J. Alstrup, M. Biancardo, H. Spanggaard, Proc. SPIE 5938 (2005) 593804.
[122] F.C. Krebs, M. Biancardo, B. Winther-Jensen, H. Spanggaard, J. Alstrup, 90 (2006) 1058.
[123] B. Winther-Jensen, F.C. Krebs, Sol. Energy Mater. Sol. Cells 90 (2006) 123.
[124] F.C. Krebs, H. Spanggaard, T. Kjær, M. Biancardo, J. Alstrup, Mater. Sci. Eng. B 138 (2007) 106.
[125] E. Bundgaard, F.C. Krebs, Sol. Energy Mater. Sol. Cells 91 (2007) 1019.
[126] M.H. Petersen, O. Hagemann, K.T. Nielsen, M. Jørgensen, F.C. Krebs, Sol. Energy Mater. Sol. Cells 91 (2007) 996.
[127] M. Andersen, J.E. Carlé, N. Cruys-Bagger, M.R. Lilliedal, M.A. Hammond, B. Winther-Jensen, F.C. Krebs, Sol. Energy Mater. Sol. Cells 91 (2007) 539.
[128] T. Jeranko, H. Tributsch, N.S. Sariciftci, J.C. Hummelen, Sol. Energy Mater. Sol. Cells 83 (2004) 247.
[129] E.A. Katz, D. Faiman, S.M. Tuladhar, J.M. Kroon, M.M. Wienk, T. Fromherz, F. Padinger, C.J. Brabec, N.S. Sariciftci, J. Appl. Phys. 90 (2001) 5343.
[130] E.A. Katz, S. Gevorgyan, M.S. Orynbayev, F.C. Krebs, Eur. J. Appl. Phys. 36 (2007) 307.
[131] G. Dennler, C. Lungenschmied, H. Neugebauer, N.S. Sariciftci, A. Labouret, J. Mater. Res. 20 (2005) 3224.
[132] G. Dennler, C. Lungenschmied, H. Neugebauer, N.S. sariciftci, M. Latréche, G. Czeremuzkin, M.R. Wertheimer, Thin Solid Films 511–512 (2006) 349.
[133] C. Lungenschmied, G. Dennler, H. Neugebauer, N.S. Sariciftci, M. Glatthaar, T. Meyer, A. Meyer, Sol. Energy Mater. Sol. Cells 91 (2007) 379.
[134] S. Schuller, P. Schilinsky, J. Hauch, C.J. Brabec, Appl. Phys. A 79 (2004) 37.
[135] R. De Bettignies, F. Leroy, M. Firon, C. Sentein, Synth. Met. 156 (2006) 510.
[136] G.C.M. Silvestre, M.T. Johnson, A. Giraldo, J.M. Shannon, Appl. Phys. Lett. 78 (2001) 1619.
[137] Y. Sahin, S. Alem, R. de Bettignies, J.-M. Nunzi, Thin Solid Films 476 (2005) 340.
[138] (a) F.C. Krebs, Sol. Energy Mater. Sol. Cells 92 (2008) 725–736, this issue; doi:10.1016/j.solmat.2008.01.013;
(b) K. Lee, J.Y. Kim, S.H. Park, S.H. Kim, S. Cho, A.J. Heeger, Adv. Mater. 19 (2007) 2445;
(c) B. Fan, R. Hany, J.-E. Moser, F. Nüesch, Org. Electron. 9 (2008) 85.

[139] G. Yu, J. Gao, J.C. Hummelen, F. Wudl, A.J. Heeger, Science 270 (1995) 1789.
[140] X. Yang, J.K.J. van Duren, R.A.J. Janssen, M.A.J. Michels, J. Loos, Macromolecules 37 (2004) 2151.
[141] S. Bertho, I. Haeldermans, A. Swinnen, W. Moons, T. Martens, L. Lutsen, D. Vanderzande, J. Manca, A. Senes, A. Bonfiglio, Sol. Energy Mater. Sol. Cells 91 (2007) 385.
[142] R.J. Kline, M.D. McGehee, E.N. Kadnikova, J. Liu, J.M.J. Fréchet, M.F. Toney, Macromolecules 38 (2005) 3312.
[143] E. Klimov, W. Li, X. Yang, G.G. Hoffmann, J. Loos, Macromolecules 39 (2006) 4493.
[144] X. Yang, J. Loos, Macromolecules 40 (2007) 1354.
[145] S. Berson, R. de Bettignies, S. Baillo, S. Guillerez, Adv. Funct. Mater. 17 (2007) 1377.
[146] K. Sivula, C.K. Luscombe, B.C. Thompson, J.M.J. Fréchet, J. Am. Chem. Soc. 128 (2006) 13988.
[147] B. Pradhan, A.J. Pal, Chem. Phys. Lett. 416 (2005) 327.
[148] J.M. Kroon, M.M. Wienk, W.J.H. Verhees, J.C. Hummelen, Thin Solid Films 403 (2002) 223.
[149] C.R. McNeill, C.J.R. Fell, J.L. Holdsworth, P.C. Dastoor, Synth. Met. 153 (2005) 85.
[150] C.W.T. Bulle-Lieuwma, W.J.H. van Gennip, J.K.J. van Duren, P. Jonkheijm, R.A.J. Janssen, J.W. Niemantsverdriet, Appl. Surf. Sci. 203 (2003) 547.
[151] C.W.T. Bulle-Lieuwma, J.K.J. van Duren, X. Jang, J. Loos, A.B. Sieval, J.C. Hummelen, R.A.J. Janssen, Appl. Surf. Sci. 231 (2004) 274.
[152] J.K.J. van Duren, X. Jang, J. Loos, C.W.T. Bulle-Lieuwma, A.B. Sieval, J.C. Hummelen, R.A.J. Janssen, Adv. Funct. Mater. 14 (2004) 425.
[153] W. Bijnens, J. Manca, T.-D. Wu, M. D'Olieslaeger, D. Vanderzande, J. Gelan, W. de Ceuninck, L. de Schepper, L.M. Stals, Synth. Met. 83 (1996) 261.
[154] H. Heil, J. Steiger, S. Kart, M. Gastel, H. Ortner, H. von Seggern, M. Stöβel, J. Appl. Phys. 89 (2001) 420.
[155] S. Gevorgyan, M. Jørgensen, F.C. Krebs, this issue.
[156] P. Madakasira, K. Inoue, R. Ulbricht, S.B. Lee, M. Zhou, J.P. Ferraris, A.A. Zakhidov, Synth. Met. 155 (2005) 332.
[157] E.A. Meulenkamp, R. van Aar, J.J.A.M. Bastiaansen, A.J.M. van den Biggelaar, H. Börner, K. Brunner, M. Büchel, A. van Dijken, N.M.M. Kiggen, M. Kilitziraki, M.M. de Kok, B.M.W. Langeveld, M.P.H. Ligter, S.I.E. Vulto, P. van de Weijer, S.H.P.M. Winter, Proc. SPIE 5464 (2004) 90.